Scalable Computing: Practice and Experience

Scientific International Journal for Parallel and Distributed Computing

ISSN: 1895-1767

Volume 23(2) June 2022

SUBSCRIPTION INFORMATION: please visit `http://www.scpe.org`

Scalable Computing: Practice and Experience

Volume 23, Number 2, June 2022

TABLE OF CONTENTS

Regular Papers:

Scalable Computing: Practice and Experience, ISSN 1895-1767, http://www.scpe.org
© 2022 SCPE. Volume 23, Issues 2, pp. 51–58, DOI 10.12694/scpe.v23i2.1975

A TRANSFER REPRESENTATION LEARNING APPROACH FOR BREAST CANCER DIAGNOSIS FROM MAMMOGRAMS USING EFFICIENTNET MODELS

PARITA OZA[*], PAAWAN SHARMA, AND SAMIR PATEL [†]

Abstract. Breast cancer is a deadly disease that affects the lives of millions of women throughout the world. Over time, the number of cases of breast cancer has increased. Preventing this disease is difficult and remains unidentified, but the survival percentage can be improved if diagnosed early. The progress of computer-assisted diagnosis (CAD) of breast cancer has seen a lot of improvements thanks to advances in deep learning. With the notable advancement of deep neural networks, diagnostic capabilities are nearing a human expert's. In this paper, we used EfficientNet to classify mammograms. This model is introduced with the new concept of model scaling called compound scaling. Compound scaling is the strategy which scales the model by adding more layers to extend the receptive field along with more channels to catch the detailed features of larger input. We also compare the performance of various variants of EfficientNet over CBIS-DDSM mammogram datasets. We used the optimum fine-tuning procedure to represent the importance of transfer learning (TL) during training.

Key words: Convolutional Neural Networks, EfficientNet, Breast Cancer, Transfer Learning

AMS subject classifications.

1. Introduction. Breast cancer is the most frequent type of cancer worldwide, especially among women, and it is also the leading cause of death. Breast cancer can be detected early, allowing for better treatment planning and a higher survival rate. The most effective techniques for early detection of breast cancer are several imaging modalities such as mammography, Breast MRI, Breast Ultrasound, and PET CT [1]. Computer-aided diagnosis (CAD) systems are being developed for the automated diagnosis of breast cancer. This system enhances the accuracy of findings and the ability to distinguish between abnormalities such as mass, micro-calcification, architectural distortion, etc. CAD systems can act as a double reader solely meant to assist a radiologist; only expert clinicians make final choices.

Deep convolutional neural networks are commonly used in various medical imaging tasks such as cancer detection, classification, and segmentation [18]. Unfortunately, training a network from the ground up can take days or weeks and necessitates a lot of computational power. The research community, on the other hand, already has an access to pre-trained networks like as AlexNet [2], VGGNet [3], ResNet [4], Google Inception Family [5], EfficientNet [6], and so on. Rather than beginning from scratch, most current research suggests leveraging pre-trained networks. On the other hand, state-of-the-art networks are built and tested on datasets that are substantially more diverse [7]. As a result, such networks' capacity and complexity may exceed the needs of smaller datasets, resulting in severe drawbacks when learning from scratch. As a result, several papers have appeared in which the authors call for comprehensive training [7]. In light of the aforementioned, we examine the performance of EfficientNet [6] using the transfer learning approach. Furthermore, we compare the performance of various variants of the EfficientNet family by commencing the training with pre-trained weights.

The rest of the paper is organized as follows: Section 2 deals with the related work in the domain. Then, in section 3, we discuss the EfficientNet model in brief. Then, section 4 presents the proposed methodology used in this work. Experimental results are discussed in section 5. We finally end with the conclusion in section 6.

*Pandit Deendayal Energy University, Nirma University (parita.ophd19@sot.pdpu.ac.in, parita.prajapati@nirmauni.ac.in).
†Pandit Deendayal Energy University

2. Related Work in the Domain. Rahman et al. [8] proposed modified versions of InceptionV3 and ResNet50. The authors have altered the output layer and added two fully connected layers. During the experiment, the first seven layers of the InceptionV3 model were frozen, and two fully linked layers were added, with the last layer being replaced with a Softmax layer for binary classification. A similar logic was applied for ResNet50. Chougrad et al. [9] investigated the significance of transfer learning and tested various deep CNN models to find the optimum fine-tuning technique. With the Swish activation function, a modified VGG16 model was proposed in [10]. Authors have shown that the modified VGG16 model with the Swish activation function delivers better accuracy than Relu activation. A comprehensive study of mammogram classification techniques of various deep learning and machine learning approaches is presented in [11]. Apart from these, Support vector machine (SVM), naive bayes , artificial neural network (ANN), and set classifiers [12] are some of the machine learning algorithms that have proven popular for the development of computer-aided diagnosis systems for breast cancer [13, 14]. Another work by Ikechukwu et al. [19] presented a comparative study of two pre-trained models, such as ResNet-50 and VGG-19, against training a model from scratch (Iyke-Net). Data augmentation and dropout regularization were employed to reduce overfitting. Authors concluded that the pre-trained models with sufficient fine-tuning were comparable to Iyke-Net, a CNN developed from scratch, with a recall of 92.03 percent.

We found that transfer learning plays a substantial role in various deep learning algorithms based on our literature review. With a modest number of datasets, this method is useful in the medical arena [15, 21]. Different existing models based on a short dataset with the CNN architecture and the transfer learning method have not been completely investigated till now. As a result, using a modified state-of-the-art CNN architecture, there is potential for additional advancement in deep learning approaches.

3. EfficientNet Model Scaling. Convolutional Neural Networks have become common in the realm of Computer Vision since Alexnet won the 2012 ImageNet Challenge. However, one of the most challenging aspects of developing CNNs is model scaling so as to improve model accuracy. This process is time-consuming and also necessitates manual trial and error until a sufficiently accurate model is generated while meeting the resource constraints [6]. The procedure consumes a lot of resources and time, and it often results in models that aren't as accurate or efficient as they could be. In response to this issue, Google published a study in 2019 that discussed a new family of CNNs called EfficientNet [6]. The authors of this paper contributed two things:

- Development of mobile-friendly baseline architecture.
- The concept of compound scaling introduces a strategy for expanding model size and maximizing accuracy improvements.

The concept of compound scaling strategy for expanding model size and maximizing accuracy improvements. Depth, breadth, and resolution are three parameters to scale the convolutional neural network. The number of layers in a network refers to the network depth. The number of neurons in a layer, or the number of kernels or filters in a convolutional layer, is related to the width. The input image's height and width are used to determine the resolution. Figure 3.1 shows pictorial representation of compound scaling. An EfficientNet introduces two rules.

- The scaled models' layers/stages will all use the same convolution techniques as the baseline network.
- All layers must be scaled in the same way, with the same ratio.

All layers must be scaled in the same way, with the same ratio. Equation 3.1 mathematically presents the definition of EfficientNet imparting these two rules.

$$N(d, w, r) = \sum_{1..s} F_i^{d, L_i}(X_(r.H_i, r.W_i, w.C_i)) \tag{3.1}$$

where w, d, r are scaling coefficients to scale width, depth, and resolution of the network; F_i, L_i, H_i, W_i, C_i are predefined parameters in baseline network. The authors offer a simple but successful scaling strategy that employs a compound coefficient to uniformly scale network breadth, depth, and resolution in a principled manner (see equations 3.2 to 3.4):

$$depth : d = \alpha^{\phi} \tag{3.2}$$

$$width : w = \beta^{\phi} \tag{3.3}$$

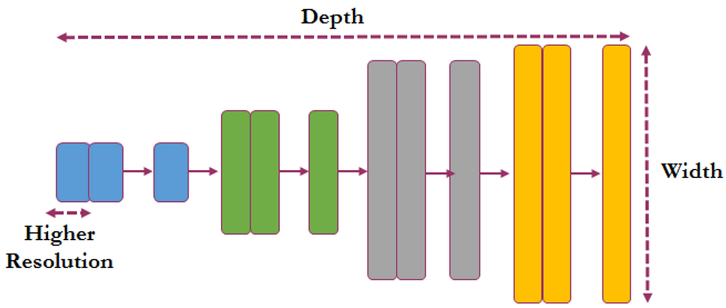

Fig. 3.1: Compound Scaling

Table 4.1: Image input shape expected for each model

Basemodel	Resolution
EfficientNetB0	224
EfficientNetB1	240
EfficientNetB2	260
EfficientNetB3	300
EfficientNetB4	380
EfficientNetB5	456
EfficientNetB6	528
EfficientNetB7	600

$$resolution : r = \gamma^{\phi} \tag{3.4}$$

With the help of grid search and by setting ϕ=1, the parameters α, β, and γ can be determined. Once these parameters have been identified, they can be fixed, and the compound coefficient ϕ increases to produce larger but more accurate models. EfficientNet B1-B7 are built in this manner, with the integer at the end of the name denoting the value of the compound coefficient.

4. Proposed Methodology. In this work, we used different versions of EfficientNet. We used TL [16, 17] approach to combat the effect of overfitting. Figure 4.1 shows the complete methodology adopted for the work carried out in this study. The TL is applied to the EfficientNet model (all versions) to classify mammograms in our work. As shown in figure 4.1, we used the recent implementation of deep neural networks that incorporates TL by using parameters of a pre-trained model for a particular task to initialize the new model with certain modifications. First, we created a base model and populated it with pre-trained weights. All the layers in the base model are then frozen by setting "trainable" as a "False". A new model is then created on top of the output of one (or several) layers from the base model. Finally, we train the new model on CBIS-DDSM [20] dataset. The classic oscillating problem is handled by varying the learning rate from 0.001 to 0.0005. The EfficientNet family has eight models, B0 to B7, out of which we used EfficientNetB0 to B5 and EfficientNetB7 in our work. Many factors control the choice of depth, resolution, and width. Therefore, the input shapes for B0 through B7 basic models differ. Table 4.1 shows the input shapes that are predicted for each model. To improve the model's performance and mitigate the effect of overfitting, data augmentation methods are also used in the proposed work. Table 4.2 shows the hyperparameters used to train all the variants of EfficientNet as well as parameters for the augmented strategies.

About Dataset: CBIS-DDSM (Curated Breast Imaging Subset of DDSM) [20] is a standardised and improved version of DDSM. The 10,239 mammographic images, with normal, benign, and malignant cases, were chosen and curated by a skilled mammographer. The images are converted to DICOM format, and the

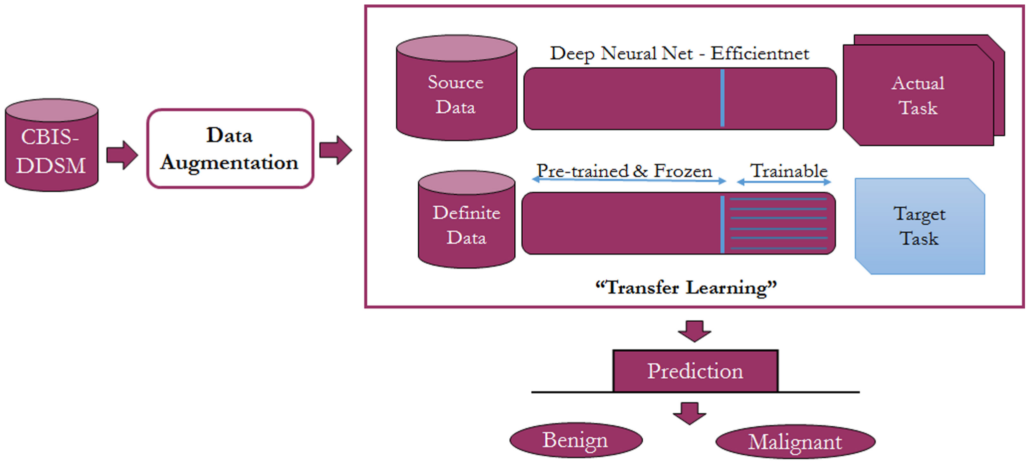

Fig. 4.1: Methodology

Table 4.2: Model Parameters for Training and Data Augmentation

Hyper Parameters for training	
Batch Size	64
Validation split	0.2
Epochs	100
Learning Rate	0.0005
Loss Function	Binary Crossentropy
Optimizer	Rmsdrop
Data Augmentation Parameters	
Rotation Range	180
Shear Range	10
Zoom Range	0.2
Fill Mode	reflect
Horizontal and Vertical Flip	True

ROI segmentation for each lesion is updated. The dataset is separated into training and testing subgroups to directly compare performance between different methodologies. Due to extensive memory usage during training time, we used 6700 images for our work.

5. Result Analysis and Discussion. We carried out experiments of the proposed model on "The PARAM Shavak system ." The system has two multi-core x86_64 CPUs, each having 12 or more cores. The GPU card used for this work is Intel Xeon Phi or Nvidia Tesla GPGPU. Moreover, the system has 64 GB RAM and 8 TB RAID-5 storage. With the default ratio of 80:20, we split the dataset into train and test random splits. The improved models are trained with 100 epochs and 64 instances each batch. In our research, we employed accuracy and loss as performance metrics. We measured accuracy and loss for all types of cases, including train, test, and validation. Figures 5.1, 5.2, and 5.3 show the training and validation performance of the improved EfficientNet models, respectively.

The validation and test accuracy, as well as the validation and test loss, for all EfficientNet models, are summarized in Table 5.1. We found that the performance of EfficientNetB2 and EfficientNetB3 are nearly identical. We set up the models so that the accuracy and loss are optimum. Early stopping was also employed to keep track of the validation loss. The best findings, as well as the results collected to the final epoch, have

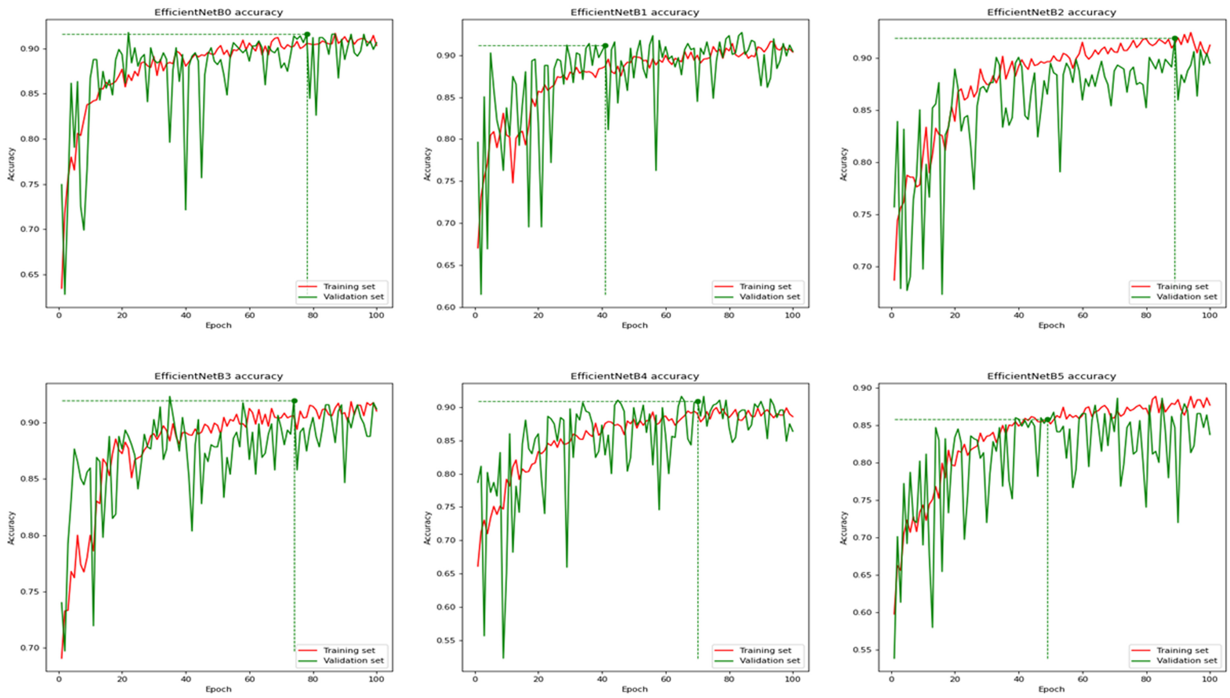

Fig. 5.1: Accuracy for EfficientNet B0 to B5

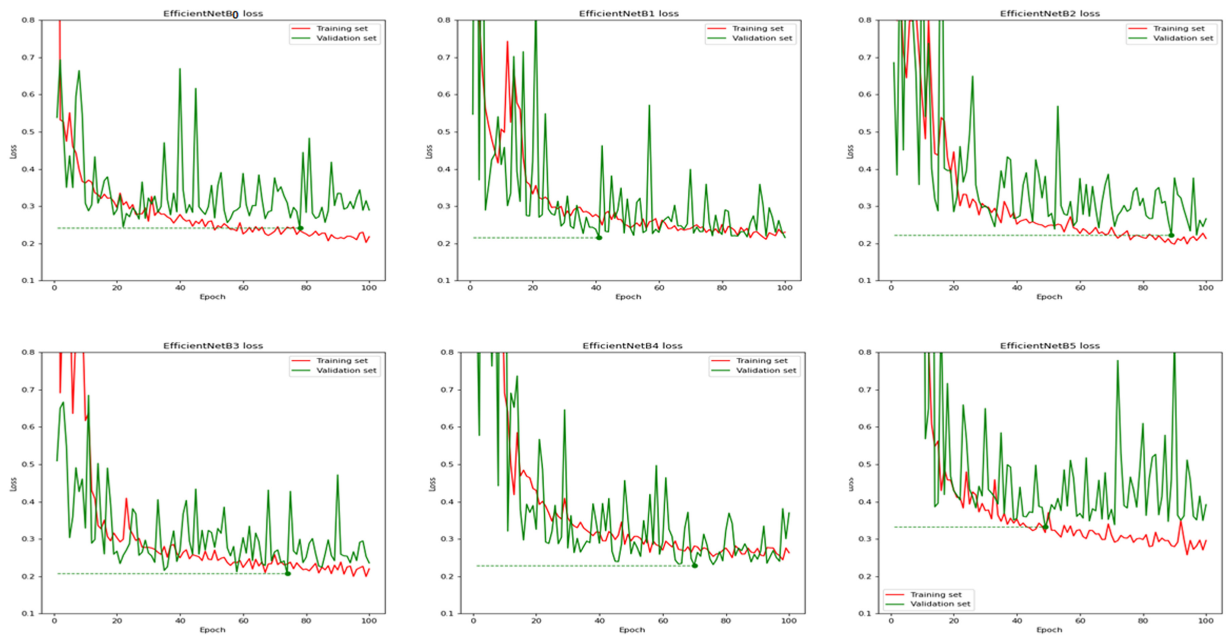

Fig. 5.2: Loss for EfficientNet B0 to B5

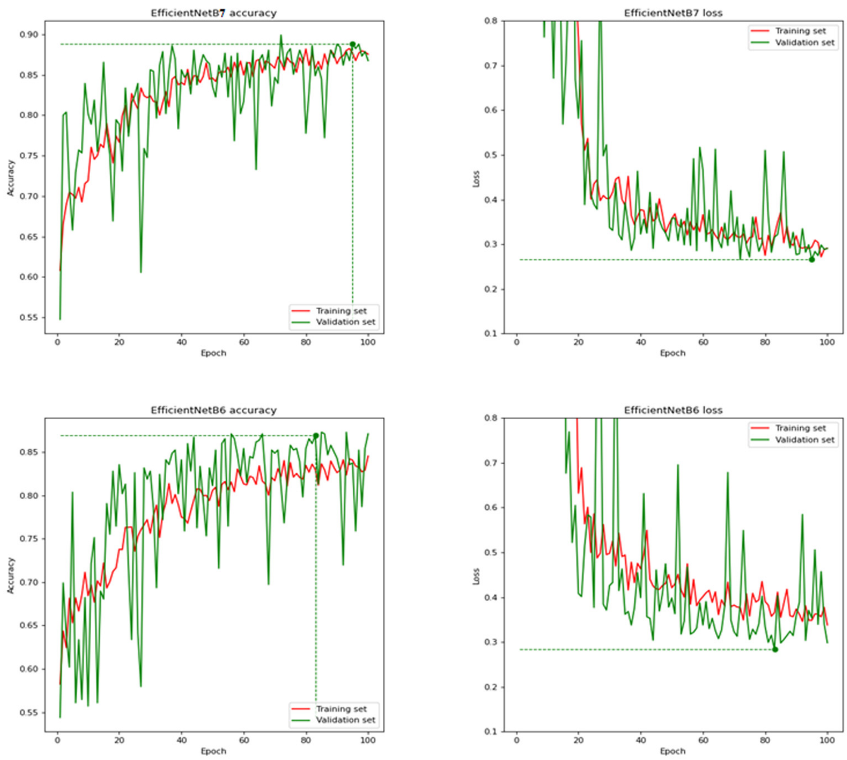

Fig. 5.3: Accuracy and Loss for EfficientNet B6 and B7

Table 5.1: Performance Measures by Various EfficientNet Models

	Validation Accuracy	**Validation Loss**	**Test Accuracy**	**Test Loss**
EfficientNetB0	0.9159	0.2413	0.8512	0.3928
EfficientNetB1	0.9121	0.2154	0.8810	0.2793
EfficientNetB2	0.9196	0.2223	0.8155	0.2734
EfficientNetB3	0.9196	0.2070	0.9018	0.2471
EfficientNetB4	0.9084	0.3699	0.8452	0.3940
EfficientNetB5	0.8579	0.3326	0.8482	0.3521
EfficientNetB6	0.8692	0.2839	0.8125	0.3888
EfficientNetB7	0.8879	0.2655	0.9018	0.2389

been reported. Figure 5.3 shows that EfficientNetB7 has the best accuracy and loss at almost the last epoch (100 for our example), while EfficientNetB6 could result into its best performance prior to the final epoch. EfficientNetB6 almost falls between EfficientNetB5 and EfficientNetB7 in terms of validation accuracy and loss. In terms of test accuracy, EfficientNetB2 and B6 are nearly equal. The optimized outcomes for the other models can be observed before the final epoch (See figure 5.1 and 5.2).

EfficientNet gets very high accuracy while using fewer parameters. A baseline network called EfficientNet-B0 was created first, and then scaled it up to create Efficient-B1 through B7. Comparing EfficientNetB7 to all other versions of the EfficienNet family, we can observe that it offers the best test accuracy and the lowest test loss. The idea behind this neural network is that larger input images necessitate additional layers, which expand the receptive field, and more channels, which enable the network to catch more fine-grained patterns on the larger images. With 600×600 resolution, EfficientNetB7 is the largest EfficientNet model that has obtained state-of-the-art performance on the datasets like CIFAR-100 and ImageNet. The outcome demonstrates that the model performs just as well on medical datasets, including the one utilized in this study.

Compound scaling is a better way to scale up neural networks. The main idea behind the compound scaling approach is the notion of balancing width, depth, and resolution dimensions by scaling with a fixed ratio. In the table 4.1, we present resolution parameters for each EfficientNet model that we employed in our research. The remaining parameters such as depth and width are predefined in the baseline network. Section 3 presents a brief discussion of the selection process utilized by EfficientNet models for all of these parameters.

6. Conclusion. It is preferable to scale up neural networks using compound scaling. The primary principle of the compound scaling method adopted by EfficientNet model family is to scale the model with a constant ratio in order to balance the width, depth, and resolution parameters. On several versions of EfficientNet, we present a transfer representation learning approach in this study. The deep neural model's classification accuracy improves when the fine-tuning approach is used. We discovered that the performance of EfficientNetB2 and EfficientNetB3 are practically equal in our tests. Furthermore, in comparison to other models, EfficientNetB3 is relatively stable in terms of validation and test accuracy. The presented approach is used for binary classification, but it can be modified to work with multi-class classification as well.

Acknowledgment. The authors express their gratitude to the Department of Computer Science and Engineering, Nirma University, Ahmedabad, for providing computing facilities for the studies.

REFERENCES

[1] Jalalian, Afsaneh, et al., *Foundation and methodologies in computer-aided diagnosis systems for breast cancer detection.*, EXCLI journal 16 (2017): 113.

[2] Krizhevsky, Alex, Ilya Sutskever, and Geoffrey E. Hinton., *Imagenet classification with deep convolutional neural networks.*, Advances in neural information processing systems 25 (2012): 1097-1105.

[3] Simonyan, Karen, and Andrew Zisserman. *Very deep convolutional networks for large-scale image recognition.*, arXiv preprint arXiv:1409.1556 (2014).

[4] He, Kaiming, et al., *Deep residual learning for image recognition." Proceedings of the IEEE conference on computer vision and pattern recognition*, (2016).

[5] Szegedy, Christian, et al., *Going deeper with convolutions.*, Proceedings of the IEEE conference on computer vision and pattern recognition.(2015).

[6] Tan, Mingxing, and Quoc Le., *Efficientnet: Rethinking model scaling for convolutional neural networks.*, International Conference on Machine Learning. PMLR,(2019).

[7] Tsochatzidis, Lazaros, Lena Costaridou, and Ioannis Pratikakis., *Deep learning for breast cancer diagnosis from mammograms—a comparative study.*, Journal of Imaging 5.3 (2019): 37.

[8] Rahman, Anas S. Abdel, et al., *Breast Mass Tumor Classification using Deep Learning.*, 2020 IEEE International Conference on Informatics, IoT, and Enabling Technologies (ICIoT). IEEE, (2020).

[9] Chougrad, Hiba, Hamid Zouaki, and Omar Alheyane., *Deep convolutional neural networks for breast cancer screening.*, Computer methods and programs in biomedicine 157 (2018): 19-30.

[10] Muduli, Debendra, Ratnakar Dash, and Banshidhar Majhi., *Enhancement of Deep Learning in Image Classification Performance Using VGG16 with Swish Activation Function for Breast Cancer Detection.*, International Conference on Computer Vision and Image Processing. Springer, Singapore, (2020).

[11] Oza, P.; Shah, Y.; Vegda, M., *A Comprehensive Study of Mammogram Classification Techniques.*, In Tracking and Preventing Diseases with Artificial Intelligence; Springer: Berlin/Heidelberg, Germany, 2021; pp. 217–238.

[12] Saxena, S.; Gyanchandani, M., *Machine learning methods for computer-aided breast cancer diagnosis using histopathology: A narrative review.* J. Med. Imaging Radiat. Sci. 2020, 51, 182–193.

[13] Pillai, R.; Oza, P.; Sharma, P., *Review of machine learning techniques in health care.* In Proceedings of the ICRIC 2019, Jammu, India, 8–9 March 2019; Springer: Cham, Switzerland, 2020; pp. 103–111.

[14] Oza, P.; Sharma, P.; Patel, S., *Machine Learning Applications for Computer-Aided Medical Diagnostics.*, In Proceedings of the Second International Conference on Computing, Communications, and Cyber-Security, Ghaziabad, India, 3–4 October; Springer: Singapore, 2021; pp. 377–392.

[15] Oza, Parita, et al., *A Bottom-Up Review of Image Analysis Methods for Suspicious Region Detection in Mammograms.*, Journal of Imaging 7.9 (2021): 190.

[16] Elshafey, Mohamed Abdelmoneim, and Tarek Elsaid Ghoniemy., *A hybrid ensemble deep learning approach for reliable breast cancer detection.*, International Journal of Advances in Intelligent Informatics 7.2 (2021): 112-124.

[17] Saber, Abeer, et al., *A Novel Deep-Learning Model for Automatic Detection and Classification of Breast Cancer Using the Transfer-Learning Technique.* IEEE Access 9 (2021): 71194-71209.
[18] Oza, Parita, et al., *Deep convolutional neural networks for computer-aided breast cancer diagnostic: a survey.*, Neural Computing and Applications. (2022) https://doi.org/10.1007/s00521-021-06804-y
[19] Ikechukwu, A. Victor, et al., *ResNet-50 vs VGG-19 vs training from scratch: A comparative analysis of the segmentation and classification of Pneumonia from chest X-ray images.*, Global Transitions Proceedings 2.2 (2021): 375-381.
[20] Rebecca Sawyer Lee, Francisco Gimenez, Assaf Hoogi , Daniel Rubin, *Curated Breast Imaging Subset of DDSM [Dataset].*, The Cancer Imaging Archive. DOI: https://doi.org/10.7937/K9/TCIA.2016.7O02S9CY
[21] Oza, P.; Sharma, P.; Patel, S.; Adedoyin, F.; Bruno, A., *Image Augmentation Techniques for Mammogram Analysis.*, J. Imaging 2022, 8, 141. https://doi.org/10.3390/jimaging8050141

Edited by: Gabriele Mencagli
Received: Jan 31, 2022
Accepted: Aug 20, 2022

Scalable Computing: Practice and Experience, ISSN 1895-1767, http://www.scpe.org

Volume 23, Issues 2, pp. 59–79, DOI 10.12694/scpe.v23i2.2025

REVIEW OF CROP YIELD ESTIMATION USING MACHINE LEARNING AND DEEP LEARNING TECHNIQUES

ANITHA MODI[*], PRIYANKA SHARMA[†], DEEPTI SARASWAT [‡], AND RACHANA MEHTA[§]

Abstract. The agriculture sector is subjected to constant challenge of yield deficit due to rising population, improper resource management and shrinking agricultural land. Advance yield estimates help in systematic planning to reduce such losses. However, prediction of accurate estimates is still an open challenge due to geographical diversity, crop diversity & crop area. Recently non-destructive approach has gained attention due to its robustness and provides easy availability of data from heterogeneous resources compared to its counterpart; destructive approach which is computational, resource intensive and hence less utilized. This paper conducts a detailed study on utilization of non-destructive approach to estimate yield taking into account, input feature, and methodology. We consider five major observations namely, data acquisition, pre-processing techniques, features, methodology, and result. Moreover, we summarize analysis of each observation, extract most prominent technique, the adopted methods, and finally recommends integration of different models that can be explored to improve accuracy.

Key words: Crop yield estimation, vegetation indices, counting, regression, segmentation, machine learning, deep learning

1. Introduction. Steep population growth has led to a rise in food demand over the last few decades. Undernourished and hunger counts have been consistently increasing as per FAO statistics [1]. Major agendas of the FAO included improving the quality and quantity and minimizing the losses of agricultural produce. Fig. 1.1(a) depicts the ratio of crop production to the population from the year 2015 to 2020, which shows an increasing trend, while crop production is not increasing as per yield requirement [2]. Fig. 1.1(b) depicts the year-wise production of major crops viz. Soyabean, Maize, Wheat and Rice [3]. Production losses and wastage is estimated to be about 600 million tons worldwide [4].

Accurate and advanced crop yield estimates are required for planning and gap analysis. This task involved obtaining potential and actual yield data of a particular crop. Potential yield y_P is obtained when a crop is grown in an ideal condition with optimal nutrient supply and an adapted environment without any stress [5]. Actual yield y_A is obtained when the crop is subjected to realistic conditions. The difference between potential and actual yield is the yield gap δy_G as shown in Equation 1.1.

$$\delta y_G = y_P - y_A \tag{1.1}$$

Destructive and non-destructive approaches were adopted to obtain actual yield value, which is still an open challenge. It depends on factors like regional crop cultivation techniques, climatic conditions, meteorological, physiological, growth factors, quality of the crop, etc. Several such factors were identified and categorized into qualitative and quantitative factors. Agrometeorological data like irrigation, soil data, climate, and soil nutrients were majorly incorporated into yield estimation models. Factors such as VI, LAI, and phenotype evapotranspiration were accommodated into quantitative data-oriented estimation models. There was a need to gather accurate agrometeorological data. Country-wise, meteorological and agricultural departments contributed to this task. These RS data obtained from the specialized sensor were also made available. The availability of diverse data led to various model designs ranging from traditional CCE to modern AI-based models. The survey focuses on the non-destructive approach adopted to calculate the yield y_A.

[*]CSE Department, Nirma University(16extvphde159@nirmauni.ac.in).
[†]Samyak Infotech, Ahmedabad,India.(drpriyankasharma.ai@gmail.com).
[‡]CSE Department, Nirma University(deepti.saraswata@nirmauni.ac.in).
[§]CSE Department, Nirma University(rachana.mehta@nirmauni.ac.in).

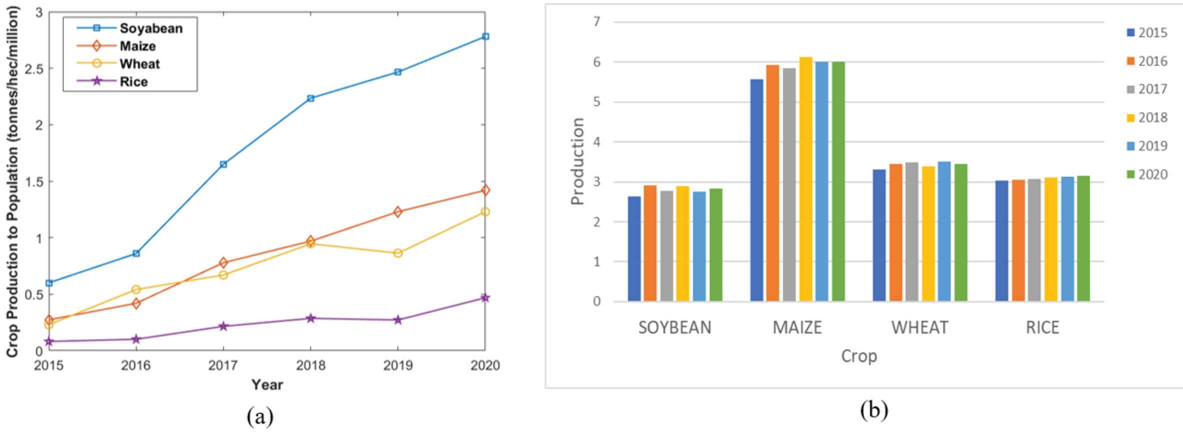

Fig. 1.1: (a) Crop production versus population (b) Year-wise crop production

Table 1.1: Comparative study of yield estimation surveys with our survey

Ref	**Summary**	**Data**				**Model**				
		A	B	C	D	1	2	3	4	5
[6]	RS with regression to estimate yield		✓	✓			✓		✓	
[7]	ML algorithms along with RS data		✓	✓	✓		✓			✓
[8]	Brief overview of ML yield model	✓						✓	✓	
[8]	Discussed ML & RS integration		✓	✓	✓		✓		✓	
[10]	ML applicability in yield estimation with climatic parameters as input		✓	✓					✓	
[12]	Summarized statistical and simulation models		✓	✓	✓	✓				
[13]	DL and counting based model	✓						✓		✓
[14]	A combination of ML and DL algorithms with major focus on ML		✓	✓	✓				✓	✓
[15]	DL and image-based yield	✓								✓
[16]	ML with specific focus on palm oil yield		✓	✓	✓				✓	
Our paper		✓	✓	✓	✓	✓	✓	✓	✓	✓

1.1. Scope of the survey. This section covers a summary of the existing review articles about yield estimation. Johnson *et al.*, considered popular ML models with ANN and regression, BP-ANN [6]. Chivasa *et al.*, conducted similar studies [7], using meteorological & environmental data and suggested to include RS data into ML model. Liakos *et al.*, reviewed application of ML into agricultural sector [8]. Chlingaryan *et al.* further explored RS with ML, stating the need for a feature-rich dataset and advanced ML algorithms [9]. Elavarasan and Vincent studied environment and climate data. They studied the applicability of unsupervised and supervised ML algorithms with climatic parameters [10]. Kamilaris & Prenafeta-Boldu explored DL architectures, and their applicability to sub-areas of precision agriculture was stated [11]. Brasso summarized statistical, and simulation models and Liu [12]. Fruit detection and localization using the counting technique to estimate was reviewed by Koirala *et al.*, [13]. Counting-based techniques was also studied by Maheswari *et al.*[15], Agrometeorological and RS by-products as input features was surveyed by Van Klompenburg *et al.*,[14]. Rashid *et al.* reviewed ML-based models along with their advantage and disadvantage [16] for palm oil prediction. A brief comparative study and our scope are summarized in Table 1.1

1.2. Contribution of the Survey. In this survey, a systematic review of yield estimation is presented. The entire paper collection is segregated into five different models based on the input data and methods. We

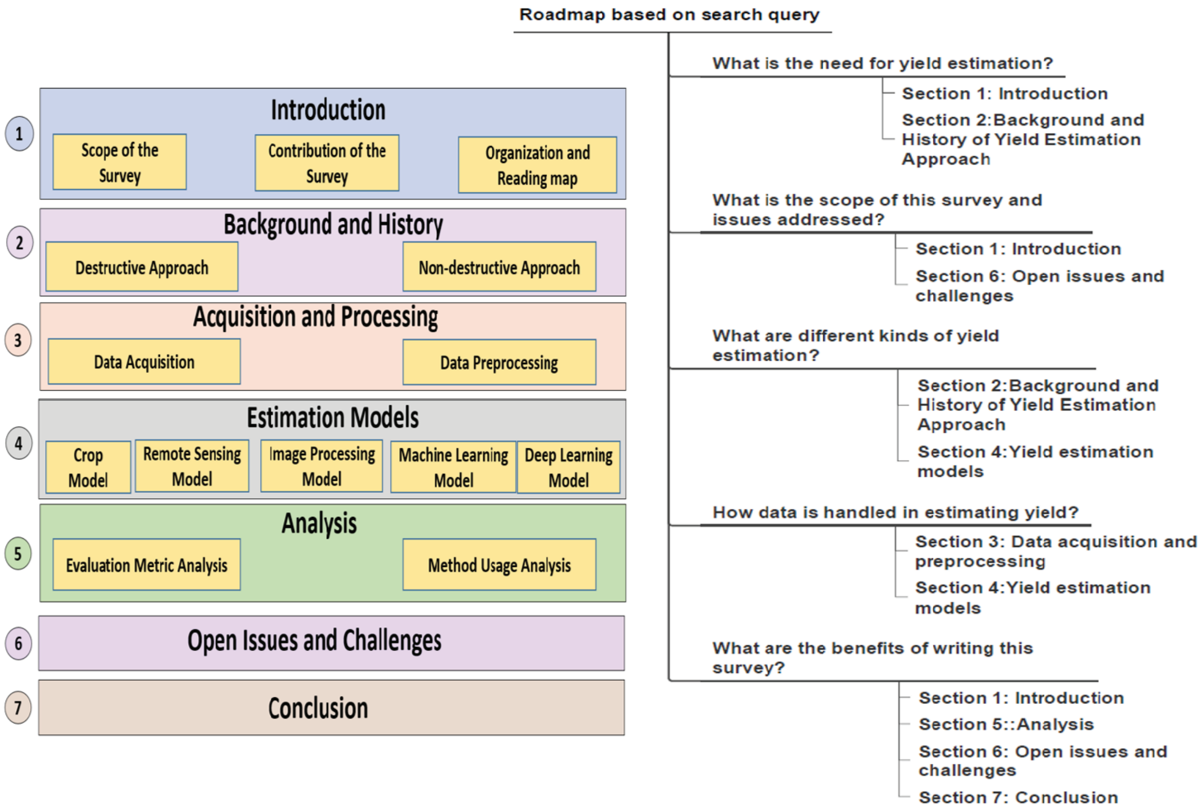

Fig. 1.2: (a): Organisation and reading map of the survey (b): Query based reading map

have highlighted the open issues and challenges faced in this research area. In line with the above statements, the major contributions made in our survey are enlisted as follows.

- A detailed description of data acquisition, preprocessing and taxonomy with comprehensive coverage of numeric and non-numeric data.
- Categorized each paper based on the input feature and the method and covered the growth of this field from traditional destructive approaches to modern non-destructive approaches.
- Presented overview of standard analysis to verify the results with their usage summary with the count. This provides an insight into the choice of evaluation metric and would aid in model designing.
- We have addressed research challenges and concluded with solution insights into open issues and challenges.

1.3. Organization and Reading Map. Standard sources such as Google Scholar, Scopus, ScienceDirect, SpringerLink and Web of Science were looked for papers. Data acquisition, preprocessing, input type, method and result analysis were significant observations that were used for selection. Based on these observations, the papers were grouped into five models: CM, RS, IP, ML and DL. Further, it was observed that the critical input features of one model were integrated into other models to obtain better results which is a significant inclusion in our survey.

A reading map consisting of the paper's complete visual layout and a query-based reading map to address readers' crucial questions is shown in Fig. 1.2. Table 1.2 list the abbreviations used in our survey.

2. Background and History of Yield Estimation Approach. Based on sampling schemes adopted, the approach is categorized into destructive and non-destructive approaches [17]. Different models were designed

Table 1.2: Abbreviations used in the survey

Abbrev.	**Meaning**	**Abbrev.**	**Meaning**
AI	Artificial Intelligence	NDVI	Normalized Difference Vegetation Index
ANN	Artificial Neural Network	NOAA	National Oceanic and Atmospheric Administration
AVHRR	Advanced Very High Resolution Radiometer	NRMSE	Normalized Root Mean Square Error
BP-ANN	Back Propagation Artificial Neural Network	RMSE	Root Mean Square Error
CCE	Crop Cutting Experiment	ROI	Region of Interest
CM	Crop Model	RRMSE	Relative Root Mean Square Error
CP-ANN	Counter Propagation Artificial Neural Networks	RS	Remote Sensing
DL	Deep Learning	RS	Remote Sensing
DVI	Difference Vegetation Index	RVI	Ratio Vegetation Index
EVI	Enhanced Vegetation Index	SKN	Supervised Kohonen Networks
FAO	Food and Agriculture Organization	SMLR	Stepwise Multiple Linear Regression
GI	Greenness Index	SNN	Semiparametric Neural Network
HRV	High Resolution Vertical	SPOT	French: Satellite Pour l'Observation de la Terre
IP	Image Processing	TCI	Temperature Condition Index
LAI	Leaf Area Index	VCI	Vegetation Condition Index
MAE	Mean Absolute Error	VHI	Vegetation Health Indices
MAPE	Mean Absolute Percentage Error	VI	Vegetation Indices
ML	Machine Learning	WDRVI	Wide Dynamic Range Vegetation Index
MODIS	Moderate Resolution Imaging Spectroradiometer	WHR	Weighted Histogram Regression
NAIP	National Agriculture Imagery Program	WOFOST	WOrld FOod STudies

and experimented with for each approach, as shown in Fig. 1.3. Each model used a subset of data gathered from heterogeneous sources. Researchers have explored several methods ranging from traditional field surveys, and CCE [18] to modern DL [82] to provide a solution. A detailed discussion of these models and the methods adopted in each model is covered in the subsequent sections.

2.1. Destructive approach. The destructive approach means clearing a portion of the field for sampling or harvesting the crop to obtain estimates. The approach is further segregated into the pre-harvest and post-harvest models. Pre-harvest model provides yield estimates before actual harvest, such as CCE. A physical field examination with a collection of samples for analysis is done in CCE [20]. Yield is estimated and extrapolated to the entire crop region during sample analysis as illustrated in Fig. 1.3. Yield details are obtained from market records post-harvest. Both methods provide accurate estimates. However, this approach is resource intensive. A considerable workforce and micro-level planning are required for CCE site identification and market surveys. Site visits and market surveys in the post-harvest method are difficult due to inherent variations in market structure, geographical diversity, and biodiversity [21]. Further, estimates are available at the later stage or after harvest, which affects the planning. Hence, the destructive approach is less used and is not covered in our survey.

2.2. Non-destructive approach. Several visual and analytical models were designed and studied using data from heterogeneous sources such as past yield data, environmental, meteorological, physiological and visual data. This approach provided advanced estimates without undergoing any destructive process such as harvesting, hence the non-destructive method. Non-destructive offers advanced estimates without experiencing time-consuming market surveys, CCE site identification and experimentation at a macro level. But is highly

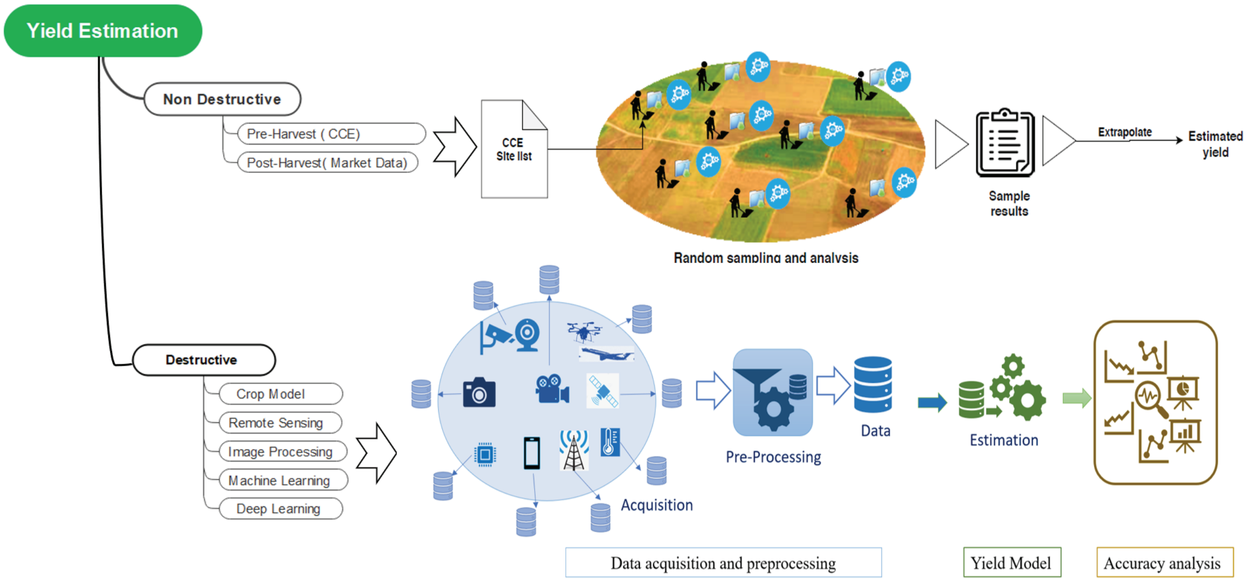

Fig. 1.3: Different yield estimation approaches

dependent on accurate data. The study was initialized with numerical data. However, the availability of data from heterogeneous sources and technological progress allowed researchers to explore the possibility of including them in yield models. The entire non-destructive approach is summarized into three generic phases as shown in Fig. 1.3.

3. Data acquisition and preprocessing. To estimate yield, data plays a vital role. This section covers the detailed taxonomy of data acquisition and processing. A brief specification of their usage in different models is also covered in this section.

3.1. Data acquisition. The data acquisition process involves data collection. Site-specific data are recorded using various devices. Gathered data is categorized into numeric & non-numeric. Numeric data is segregated into meteorological, environmental and economic [22], [23]. The data combines categorical or continuous data and provides qualitative and quantitative features that can be used as input. Temperature, humidity, sunshine, and precipitation are widely used meteorological data. Environmental parameters include soil properties, crop type, harvest information, acreage, phenology, & irrigation. Economic data includes market statistics such as trading prices and harvest information about crop gathering and production. Machine learning [39], [40], crop models [41] widely use this data for estimate prediction.

Non-numeric data include images and remote sensing data products. RGB images acquired from the camera are used in image processing and deep learning models [42]. Specialized cameras such as LED [43], thermal [44], and monocular high-resolution camera devices [45] were used to capture images. Other non-numeric data are acquired from remote sensors. The most widely used remote sensing products were NIR, R(Red), and B(Blue) bands to compute values like NDVI and EVI. Data was gathered from various satellites with remote sensors such as SPOT [46], MODIS [47], Terra and Aqua [48], Landsat [49] and IRS [20]. The computation of NDVI [50] and EVI [51] for MODIS data is shown in Equation 3.1 and Equation 3.2 where βNIR, βR, βB and G represents NIR, R, B band and gain factor respectively. A sample image was acquired from earth explorer, and VI were computed. Apart from these AVHRR NOAA [52], hyperspectral imagery [53] and multispectral images [39] were also used. Fig. 3.1 illustrates the taxonomy of data.

Table 3.1: Data acquisition and preprocessing details

Model	Dataset source	Type of data	Preprocessing techniques
CM	[66]-[69]	Meteorological, environmental, economical	Recalibration, ensemble, Kalman filter, calibration of data using standard equations, atmospheric corrections, normalization
RS	[66], [70]-[72]	Environmental, image	GA for optimization, radiometric corrections, atmospheric corrections, NDVI, LAI, EVI calculation, spatial sampling, recalibration of parameters, spectral clustering, ROI extraction, manual detection of boundary mask.
IP	[43], [44], [59], [80]	Image, economical	Color conversion, grey scaling, shape analysis, segmentation, color, texture detection,edge detection, thresholding, histogram processing, histogram equalization, blurring, laplacian, sobel, symmetry analysis
ML	[73]-[76]	Meteorological, environmental, economical	Replacing missing values by mean, median, removal or merging certain column data, normalization (Z-score, mean, standard deviation)
DL	[66], [76]-[79]	Image, economical	Pixel annotation, spectral processing, cropping ROI, annotation, segmentation of pixel, augmentation, PCA, histogram processing

Several datasets are available as specified in the dataset source column of Table 3.1. Meteorological, environmental and economic data can be obtained from these sources. Entire data or a few subsets of features after required preprocessing can be used in CM, RS and ML models. IP and DL model mostly uses image data. Due to the expensive data gathering process, most of these data are unavailable as open access.

$$NDVI = \frac{\beta NIR - \beta R}{\beta NIR + \beta R} \tag{3.1}$$

$$EVI = G\frac{\beta NIR - \beta R}{\beta NIR + 6\beta R - 7.5\beta B + 1} \tag{3.2}$$

3.2. Data preprocessing. The data had to be preprocessed for several reasons, such as missing values, outliers, etc. Crop and ML models used numerical data such as climate, weather information, soil data, and meteorological data. These data were obtained from standard data sources released by country or state such as USDA, IOWA [55], Illinois [40], Minnesota university [56] etc. The data obtained from such sources might contain missing data or need to undergo recalibration. Data normalization techniques such as Z-score, mean, and standard deviations [22] were used to fix the values in the required range. Atmospheric corrections filters such as Kalman filters [55], [57] are also applied numeric data. RGB to HSV color conversion [42], reshaping [58], resizing, grey scaling [59] are some of the techniques applied to images. Apart from this, segmentation using colour, texture [59], and watershed algorithm [42] were also applied to separate ROI from the image. Preprocessing remote sensing data is essential due to the inherent complexity of data and its acquisition process. Recalibration [60], radiometric, atmospheric [46], spatial and spectral [53] corrections were applied before using the values. Since the image acquired spans a large area, ROI extraction, manual demarcation, and spatial sampling [61] were applied. GA [62] was used for optimal parameter selection on data gathered from sensors. Most deep learning models require an image dataset with a large sample size for model training. Augmentation techniques [63] helps to enhance dataset size. Remote sensing (RS) data was integrated into a deep learning model. However, the data had to be preprocessed using techniques such as histogram processing [64], pixel annotation [82]. RS data was segmented using spectral clustering [65] and ROI extraction. Table 3.1 summarizes the data acquisition techniques, a few dataset sources and preprocessing techniques widely adopted in the research work.

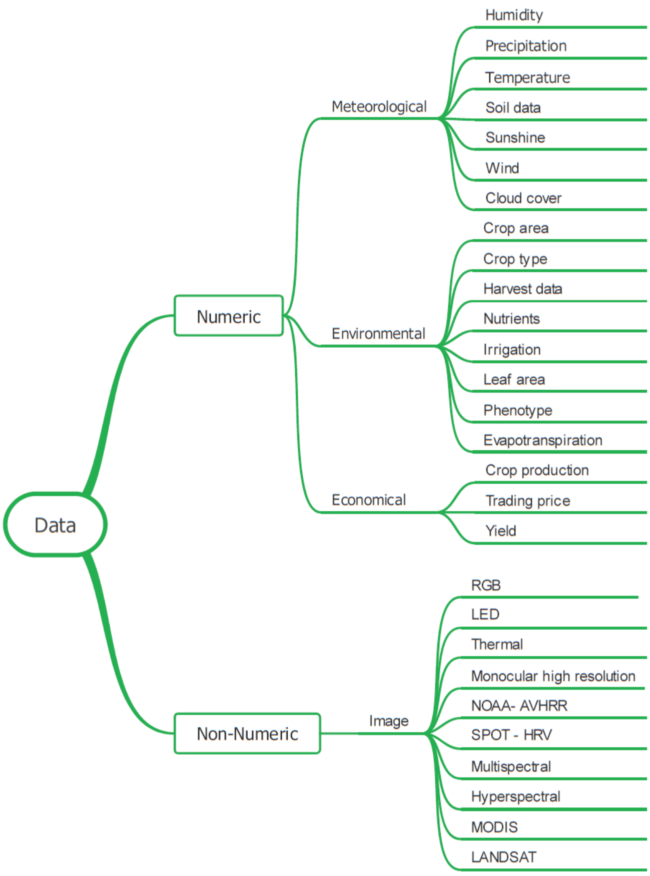

Fig. 3.1: Taxonomy of Data

4. Yield estimation models. Several methods are tried depending on the features extracted from different sources. The taxonomy of modes is shown in Fig. 4.1. Each technique is explained as it evolved in technological advancement.

4.1. Crop Models. The crop model estimation involves two mathematical models, viz. qualitative and quantitative. Crop models can be categorized as statistical or simulation-based, depending on the input. Statistical estimation models accept a set of agrometeorological data as an input into a statistical regressor to estimate yield. However, the past few decades have witnessed wide variations in climate and soil structures, impacting the estimated yield. Statistical models failed to incorporate this dynamic aspect. To overcome this, qualitative features such as soil, weather, phenology with other infield observations are incorporated into simulation models. Plant biomass and yield were generated as an output by these models. In [83], environment and growth-related parameters were used to estimate yield; the study was conducted at geographical sites with local weather station data. Experimental observations concluded that there could not be a global optimized model to estimate yield for all crops. Region-wise new models of existing models should be developed. Production and crop growth analysis was done in the WOFOST model [84]. The CERES-Maize water balance model experimented with [85] under varied weather and soil conditions in the Netherlands. Input data comprised crop species, soil profile, fertility, physical properties and historical crop yield. Initially, SUCROS [86] model studied growth under sufficient water supply and nutrients. This model did not consider growth inhibitors such as pests, diseases and weeds. Variants of this model integrated other data such as SPOT, aerial images and

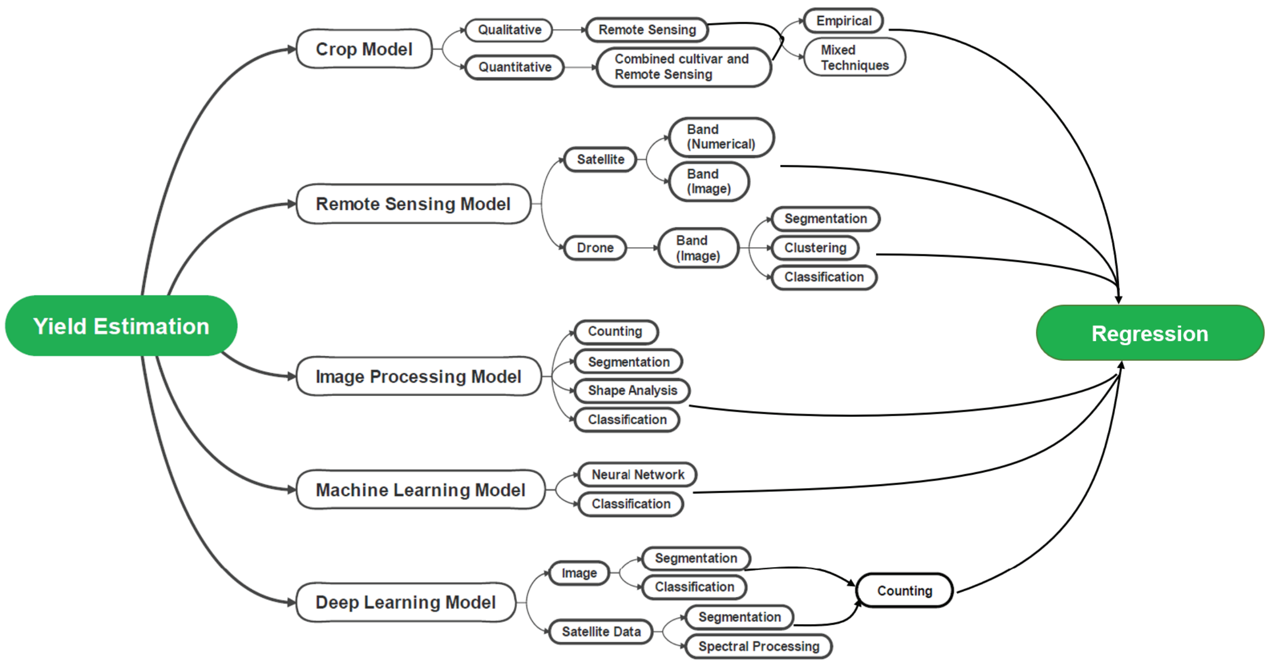

Fig. 4.1: Taxonomy of methods

remote sensing data to improve the accuracy of the model [60] [87].

A comparative study was conducted between SUCROS2 and SAIL [88] model. These models used SPOT and aerial photos to calculate leaf area; it is an early study of integrating remote sensing data into the crop model. Irrigation and Nitrogen related studies were conducted in designing the VSM model [89]. Plant density and mean daily solar parameters are included in it. Similar studies were conducted between CERES and CroySyst model in Indo-Gangetic plains. In [90] with CropSyst gives better results in the Indian subcontinent scenario. SBOCM [41] integrated geographical data from the weather station in China and the SVR method to estimate crop growth at various stages. Upscaling of AquaCrop model with RS data used to compute crop canopy and biomass was used in AquaCrop-RS [91] model for regional yield. Table 4.1 includes the summary of crop models.

4.2. RS model. Aerial and RS images were mainly used for land cover, crop classification, etc. However, certain features extracted from these images provided qualitative parameters which were integrated into yield models. The frequency of data capturing and a good resolution have allowed researchers to design a model to incorporate them. Several parameters could be calculated with the captured spectral band [92]. A subset of these calculated or calibrated values played a significant role in yield estimation models. The plant absorbs energy during photosynthesis as per plant physiology. IR and NIR bands capture this qualitative feature, indicating plant health and growth process. [61] stated the usage of RVI and NDVI data to estimate crop yield along with field survey data for the crop in India. NDVI calculated from Landsat and IRS-1A and IRS- 1B band assisted in CCE site identification leading to higher accuracy in the yield model [20]. Evapotranspiration (ET) data computed from (RS) was used in the SWAP model to recalibrate soil water content managing parameters which widely assisted in increasing yield [49]. A combination of soil moisture and LAI was integrated into the DSSAT-CSM model [55] which was unsuccessful due to discontinued satellite services. Early studies showed a linear correlation between GIN values acquired from Landsat in the US and yield estimates when integrated into the Agromet model [93]. In another paper greenness value obtained from Landsat and AVHRR data was used to generate yield estimates [94].

4.2.1. RS data used in other models. Recalibration of LAI using SPOT/ HRV data was used in the SAFY yield model [46]. In another work, LAI calculated from Landsat 7, and 8 and Sentinel-2A were assimilated into the WARM model [57]. WOFROST-PROSAIL model used KS reflectance algorithm with MODIS surface reflectance. The highest accuracy was achieved when KS reflectance values were used [47]. VI product of MODIS and LAI products was used in the CSM-CERES model for estimating yield with a conclusion that only half year product is sufficient to estimate yearly produce [62]. RS data was also used to estimate grassland biomass [95] in regions such as Ireland. Another product of MODIS, DVI was used at the national and further at the subnational level capturing extreme weather conditions [48].

The growing popularity of AI and ML led researchers to explore the possibility of using them to solve the yield estimation problem. SKN, CP-ANN and XY-F algorithms were used along with NDVI [23]. Spectral clustering of ROI into tomato and non-tomato was done using aerial images captured from a UAV. SOM and EM for clustering were used, and EM gave better results [65]. Linear regression with NDVI was used in [96]. VHI, VCI, and TCI computed weekly for almost two decades (1982- 2004) using NOAA-AVHRR were used in PCR [52] to estimate crop yield. Table 4.2 summarizes the RS yield model.

4.3. Image processing model. Several methods depending on the image source and the image acquisition mode were experimented with to obtain a yield estimate. Color, contrast, texture, and shape can be input features. Image processing techniques are used to extract these features from images. Usually, images are captured in broad daylight with maximum sun exposure using normal handheld cameras [42], [59] and mobile cameras [58]. Images captured under a controlled lighting environment using the specialized LED camera at night to avoid errors due to illumination effect [43] were also experimented. A different set of input images captured from different devices such as thermal camera [44] monocular high-resolution camera [45] was also tried. The manual image capturing was difficult due to various conditions such as large crop areas, repeated site visits at a specific time, etc. This process was automated using aerial vehicles and satellite payloads. Specialized vehicles such as UAV [65], [74], computer vision integrated autonomous vehicles [45] were used. A combination of thermal, multispectral and RGB image data captured and features extracted from them were used in another image processing-based yield model [74].

Color is an important feature that can be used in designing a yield model. Colour format conversions such as RGB to HSV were also explored to improve efficiency [97]. Experiments were conducted on trees with objects of high or meagre contrast [45], [42], [59], [98] against green foliage. The work in [99] discusses correlations such as count and weight, size and weight, and area and weight using a grape cluster as a case study. These correlations are essential while using count to estimate yield. Table 4.3 summarizes different yield models based on image processing.

4.4. Machine Learning Model. ML in AI is widely used for yield estimation. Widely used ML models include simple feed-forward neural network (NN) [101], back-propagation [22], [40] and NN.

Meteorological, environmental, and market pricing were widely used for training NN [22, 102]. SNN (a variant of NN) with panel regression using environmental features were also tried [102]. ENN gave better results when compared with BPN with different input features [22]. KNN, ANN [39], [102] used different parameters for estimation. C4.5 [104] was also used to focus on GUI design for illustrating climatic variations and estimation. GA was used for selecting optimal input features that could maximize yield estimation using BP-ANN [40]. SMLR with feed-forward NN was designed to model the relation between soil parameters, climate, and yield [101].

Table 4.1: Summary of crop model

Ref	Method	Input feature	Output	Evaluation metric	Summary	Open issues
[60]	SUCROS	SPOT, leaf area, atmospheric data	Potential growth under ideal conditions	RMSE	RS with data re-calibration & modelled potential growth	Data availability constraints
[85]	Carbon Balance + CERES-Maize water balance	LAI, meteorological, soil	Water content, expanded leaf, aerial phytomass	RMSE, R^2	Growth related parameters with water content, leaf expansion, phytomass	Limited & missing environment data, Early work
[86]	SUCROS-87	Sunlight, temperature, leaf area,	Potential growth rate	R^2	Pest, disease-free growth model	Potential model suitable under ideal conditions.
[91]	AquaCrop-RS	Soil, climate, NDVI, irrigation, canopy coverage, biomass	Yield and other simulated units	RMSE, RE, NRMSE	Integration of calculated canopy coverage, biomass from RS data into model.	Missing validation with the latest data.
[41]	SBOCM	Meteorological database of China	Rice development, Rice Yield	RMSE, RE	Estimates 1-year rice productions with meteorological RS data	Missing economic parameters
[55]	EnKF-DSSAT-CSM-Maize	Soil moisture, yield, weather, leaf area	Yield with different data assimilation	R, MBE, RMSE	Inclusion soil moisture, leaf area, data acquired from remote sensing	Discontinued satellite & data unavailability
[90]	CERES - Wheat and CropSyst	Weather, soil, plant phenotype	Status of crop and soil, Growth, Environment and stress	MAE, RMSE	Yield model comparison with increasing nitrogen supply	Geographical constraints and location dependency
[89]	VSM	Irrigation, Nitrogen	Potential yield of rice grains and biomass	R^2	Yield model with minimum input parameters	Missing important environment data
[87]	SUCROS2 and SAIL	SPOT, photos, atmospheric data	Potential yield with and without assimilation.	RRMSE	Integration of RS and aerial photos into the model	Model complexity and data acquisition difficulty.

Table 4.2: Summary of RS model

Ref.	Method	Band	D.A.	Res.	Period	Output	EM	Summ.	O.I.
[93]	Linear regression	Landsat Spectral Band	GIN data computed	10m	9 day cycle: 1978-79	Estimated & observed yield difference	Yield difference	Integrated GIN & Agromet model	Delayed yield data generation.
[94]	Linear regression	GI from Landsat NOAA-AVHRR	Landsat NOAA-6 AVHRR data	1 km	1981 year data	linear relation between GI & yield	R	Study of yield and GI	Early work. Missing other RS parameters
[20]	Linear regression	Radiance in NIR and R	IRS 1A, 1B Landsat LISS-sensor	Not considered	22 days	CCE site & yield estimation	R, SE	CCE site and yield using RS data	Limited inputs and no crop phenology
[49]	SWAP with GA for assimilation	ETM+ sensor 8 bands	Landsat7 ETM+ images	Not specified	Feb 4 & March 8, 2001	Yield under irrigation scenarios	Yield difference	RS with CM, yield with different irrigation scenarios	Missing environmental data
[52]	PCR with VHI, VCI and TCI	AVHRR, NOAA GVI, NIR, IR	NOAA AVHRR	Not mentioned	1 week (23 yrs)	Yield compared with USDA data	MAE, RMSE, R^2	Used NOAA AVHRR data	Large areas without much geographical variations.
[62]	CSM-CERES maize with LAI & VI	Blue, Green and NIR	MODIS	1Km	16 days	Included VI and LAI data as parameters	RMSE	Showed half year values are sufficient	Discontinued satellite and cloud contamination
[23]	Ortho-rectification, reflectance & calibration	Green, Red, NIR	MODIS	30m	8 day	Estimate soil properties	Accuracy	RS, ML integration	No environmental data & generic study
[65]	Spectral clustering Spatial segmentation	Red Green Blue	UAV	NA	NA	Matured stage detection	Recall Precision, F measure	Detected green and red tomatoes effectively.	Missed counting and calibration of results
[95]	MLR, ML ANN and ANFIS	Blue, Green and NIR	MODIS terra (Q1 & A1)	250m, 500m	8 day	VI values and raw band values	RMSE R^2	Statistical & ML were used for estimation	Dataset size, Data quality
[46]	Linear regression	Red, IR, Green, MIR	SPOT 4,5	5:10m, 4:20m	21 days	Correlation of estimated & measured yield	RMSE R^2	CM with LAI from SPOT	Data availability, cloud cover & recalibration

Table 4.2 continued from previous page

Ref.	Method	Band	D.A.	Res.	Period	Output	EM	Summ.	O.I.
[96]	Linear regression	Red, NIR	Terra MODIS & Landsat 5,7	30m	8 day	Yield estimated compared with USDA data	RMSE	Estimates for 7 crops with annual variations	Missing physiological & environmental data
[57]	Use of LAI into WARM rice model	Not mentioned	Landsat 7,8 and sentinel-2A	30m	2014-2016	Estimates with & without use of LAI data	MAE RRMSE	RS(LAI) used in WARM model gave better results	Recalibration issues, prevent study of in-field yield variation
[47]	MODIS, Landsat & synthetic KS into WOFROST-PROSAIL	MODIS: 1-7 band	MODIS and Landsat 5, 8 reflectance	30m	8 days	Assimilated results with different reflectance products	RMSE R^2	RS with synthetic KS yielding better results	Getting optimal value & data calibration is tedious
[48]	Linear regression with DVI from MODIS	Red and NIR band	Terra & Aqua satellites	1Km	2001-2917	Winter yields with additional low yields at extreme weather conditions	R, RMSE	Captured low yields due to extreme weather conditions	Unable to incorporate other weather extremity
[100]	Random Forest with VI from MODIS	NIR, R	MODIS	231.7m, 463.3m	8 day, 2000-2018	Yield estimates	RMSE, R^2	Different VI was computed & used	Suitable for rainfed region with high yield

Terms Ref.:Reference, Summ.: Summary, Res.: Resolution, E.M.: Evaluation Metric, D.A.: Data Acquisition, O.I.: Open Issues.

Table 4.3: Summary of image processing model

Ref.	Method	Device	Dataset	Output	EM	Summ.	O.I
[44]	RGB conversion and image detection	Thermal image camera	120 images	fruit diameter estimates & count	Difference	Thermal data for counting	Missed hidden objects
[45]	Segmentation, HSV with geo-tagging, counting	Monocular camera over autonomous vehicle	Single image for counting	Segmented object with counting to estimate yield	Error (Difference)	Different acquisition method	Expensive cannot handle object clusters.
[59]	Shape analysis, SVM & Segmentation	camera	100 random images	Count classified object	Accuracy	Classification & counting in outdoor environment	Occlusion, illumination were not handled
[98]	Detection (radial symmetry), clustering & counting	Camera	Sample size not specified	Correlation between count & weight after harvest	R^2	Count, weight correlation of grape cluster	Occlusion not handled
[43]	Night image pixel segmentation	LED camera & night image	Tree:41 images: 141	segmentation & count	Accuracy	Approach avoids illumination effects	Missing object localization
[97]	HSV conversion, thresholding, histogram equalization, spatial filter Gaussian blur	Camera	Tree:591 Images:1182	Object detected, count & time	Mean, R^2	Less error for green objects & green background	Complex preprocessing
[58]	Canny edge detection, segmentation, classification & counting	Mobile camera	Dataset: 4300 images	Classified ripe, semiripe, unripe object & count	R^2	Low cost, ML to compute yield	Blurring of images during capture
[42]	HSV conversion, thresholding, color detection, watershed segmentation, blob counting	camera	Tree: 21 Image: 84	Segmented object and count	R^2	Counting based algorithm	Single tree was taken into consideration for the study
[74]	Image stitching, geotagging with different features	RGB, thermal, multispectral	Single image from each device	Yield estimated using regresso	R^2, RMSE	Different features into yield model	Complex and expensive process

Ref.: Reference, EM: Evaluation metric, Summ.: Summarization, O.I.: Open Issues.

Table 4.4: Summary of Deep Learning Model

Ref.	Method	Dataset	Output	EM	Summary	Open issues
[63]	R-CNN, ZF net, VGG16 Augmentation: Flip, scale, flip-scale & PCA	PASCAL-VOC	Ground truth vs count by network	F1 Score	Augmentation was used to enhance dataset size.	Error in ground truth labelling & missed detecting few in a cluster.
[54]	LSTM, CNN and Gaussian Process pre-processing: Histogram generation	MODIS multispectral data	Yield estimation through regression	RMSE MAPE	Integration of RS data into DL	Computationally complex with extensive training & preprocessing time
[106]	Modified Inception-Resnet A	Training: 24000 Testing:100	Linear regression based on counting	MSE	The algorithm handled partially occluded image, shadow, moderate overlapping	Synthetic images with missing data for unripe objects
[64]	Transfer learning with LSTM, Pre-processing:Histogram & bin generation	MODIS	Regression NDVI, Band modes	RMSE R^2	Transfer learning with RS data to estimate yield	Data-dependency, issue related to specific crop data availability
[53]	Spectral processing, tree detection, CNN for identification and counting	Hyperspectral camera 494 tree images	Field count vs estimated count	R^2, RMSE	Hyperspectral sensor data used in the deep learning model	Occlusion problem, complex model due to large number of bands
[107]	DNN author designed	Syngenta crop challenge 2018 dataset	Estimated yield, check yield and yield difference	RMSE	Environment with genotype data were used for estimation	Complex model & hard to get a biological insight testing hypothesis
[82]	CNN with semantic segmentation	Image:40, Patches:11096 Testing: Image:4 Patches:1500	Manual vs system-generated count	Precision Recall F1-Score Accuracy	Resolves problems faced in image processing	Considers only one side of image. Multiple side images may lead to duplicate counting.
[108]	DNN preprocessing: fusion of features from multimodal data	Author generated thermal, multispectral and RGB images	Regression: Random forest, SVR, PLSR, DNN-F1 & DNN-F2	RMSEP, R^2	Multimodal feature fusion with data gathered from multiple sensors boarded on a UAV	Complex data gathering and preprocessing techniques. Compute intensive process.

The calendar day model against thermal was modelled to estimate yield in [103] as there were greater variations in temperature conditions. Within a year, spatial changes and weather were studied using BPNN [105]. Table 4.5 summarises various ML-based yield model.

Table 4.5: Summary of ML model

Ref	**Model**	**Input features**	**Evaluation metric**	**Description**	**Open issues**
[40]	BP-ANN	Yield, weather, soil details, phenology	RMSE, Accuracy	Studied fertilizer & rainfall with input parameter combinations	Missing weather patterns, history and regional data.
[101]	NN, SMLR	Soil data, yield, temperature, rain	R^2	Quantifiable relations between climate, soil & yield.	Overfitting & need more data on climate
[105]	BPNN	14 factors (site, topography, weather, soil)	RMSEP	Used BPNN & major patterns were captured	Missing input feature selection technique
[103]	ANN, k-NN, MR	Growth, reproductive stage	Accuracy	Calendar-oriented estimation	Limited input features
[104]	C4.5	Cloud, rainfall, temperature, yield	Average Accuracy	GUI for ease of usage. Climate changes were a major factor	Missing environmental data.
[22]	BPN, ENN, regression	meteorological, environmental, economical	Error rate	reduction in error rate	Optimal architecture was not fixed.
[39]	MLR, RF, SVM, K-NN, ANN, WHR	Agrometeorological, RS, economical data	RMSE, MAER	overall harvest with optimal seed selection	Unbalanced & missing environmental data
[102]	SNN, Panel Regression	parameters: environment, economic, irrigation	MSE	climate change impact on yield	Missing site-specific data & warmer climate conditions

4.5. Deep learning model. DNN has gained attention for solving yield estimation problems through regression analysis. Clustering and segmentation architectures are also used along with regressors to identify or extract ROIs. The ROI's were further processed to estimate the count of objects being studied. These outputs were then fed to the regressor designed for yield estimation. Deep architectures need a large dataset with a high variance to train the network. Usually, augmentation techniques such as flip, scale, PCA augmentation were used to increase the dataset size [63]. A modified inception-ResNetA architecture was used to count ROI in the image with Adam optimizer and Xavier weight to initialize the network [106]. PASCAL-VOC data set was used to identify and count from the image to estimate against ground truth [63]. DNN was used by the winners of the Syngenta challenge 2018, wherein the data set provided was used to estimate corn yield [107]. CNN-based semantic segmentation with counting technique was also used [82]. Hyperspectral and multispectral images obtained from RS or specialized cameras were available for studies. The paper discussed a preprocessing technique in which multispectral data was processed, and histograms were generated. These histograms were fed to CNN, and LSTM was integrated with a GP. A combination of CNN, LSTM and GP was also tried in [54], [64]. In another approach, spectral processing and CNN for ROI identification were experimented with using hyperspectral image (HSI) [53]. Multimodal fusion of data from different sensors captured using a UAV experimented. The extracted features were concatenated and fed as input to DNN, which was used as a regressor to estimate yield [108]. Table 4.4 list the details of DL methods in crop yield estimation.

5. Analysis. The critical part of estimation is the analysis of model-generated output with actual data to ensure the correctness of estimates generated. This section covers the evaluation metric and methods that are widely used.

5.1. Evaluation Metric. The wide methods utilized in the literature for accuracy and performance analysis are RMSE, R^2, RE and Accuracy. It was difficult to identify common evaluation metrics with benchmark values as different methods were used with different input parameters across different models. Example CM and RS models were used for rice yield estimation. However, RMSE, RE [41] MAE, RRMSE [57] and R^2 [89] with different output values were used for result analysis. This is an open issue that needs to be addressed. Hence, metric usage was considered in our study for various models. Fig. 5.1 shows the graphical representation of the metric evaluation usage across five different models considered in the survey. The most important metric having wide acceptance for evaluation has been kept initially. It also shows that the RMSE and R^2 are acceptable evaluation metrics for all five models.

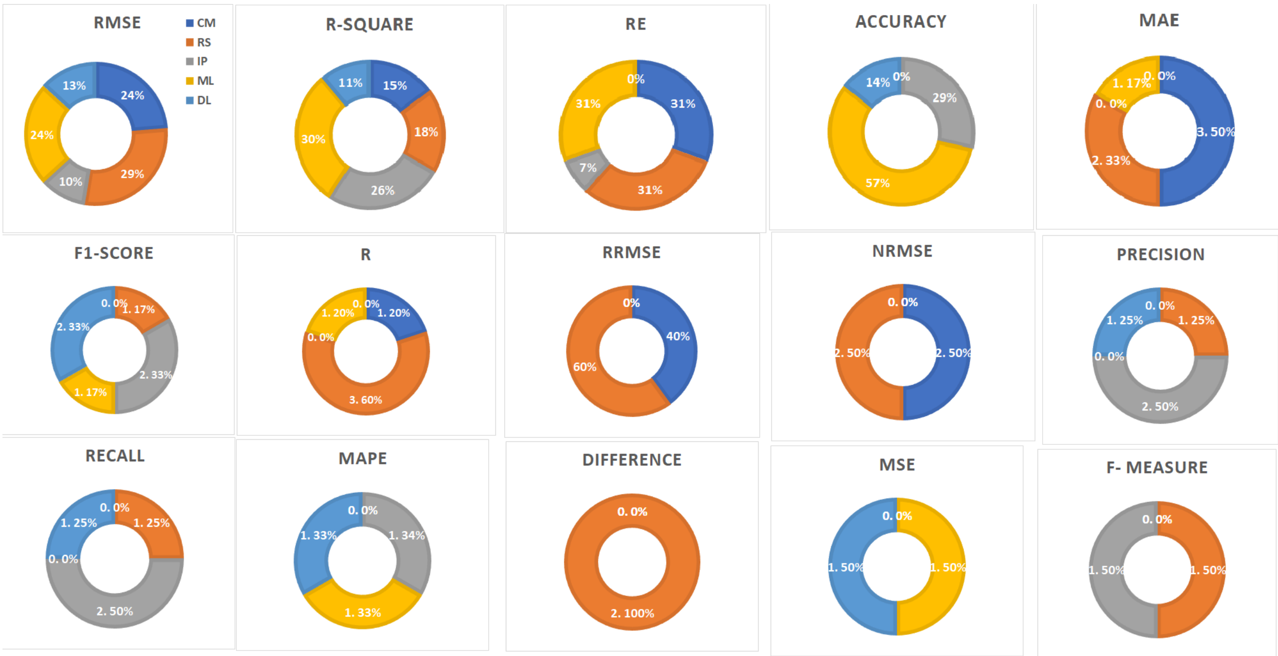

Fig. 5.1: Percentage distribution of prominent evaluation metric across 5 yield models

5.2. Method usage. We have implemented ML techniques such as SVM, segmentation, classification, clustering, K-Means, KNN, LSTM, Random Forest, NN, DNN and CNN for yield estimation. These techniques are based on statistical analysis and regression. Regressors were used in all five models. SVM in CM, IP, ML model. Segmentation in RS, IP, DL model. Classification in IP, ML, DL model. Clustering in RS, IP, DL model. K-Means and KNN in IP, ML model. LSTM in RS, DL model. Random Forest and NN in RS, ML model. DNN and CNN in DL models. It is quite clear that regression-based methods are predominantly used for yield estimation. Fig. 5.2 shows detailed usage distribution of method used across all models.

6. Open issues and challenges. This section discusses the open issues and challenges of the yield estimation models. Specific issues are common to few models.

6.1. Data related issues. A major challenge is data availability. The unavailability of historical data to train or design the model is a significant issue [87]. National or global scale data gathering is essential to test the correctness of a model developed at the regional level [52]. Satisfying this requirement is difficult due to economic and government policies laid by nations. Hence, synthetic data are generated and used while designing and testing the estimation model. This may produce incorrect results over real data [106]. Further, RS depends on satellite services to gather the required data. Discontinuity of satellite services affects the model under design or deployment [62]. RS and ML models could provide better results compared to CM. However, these models

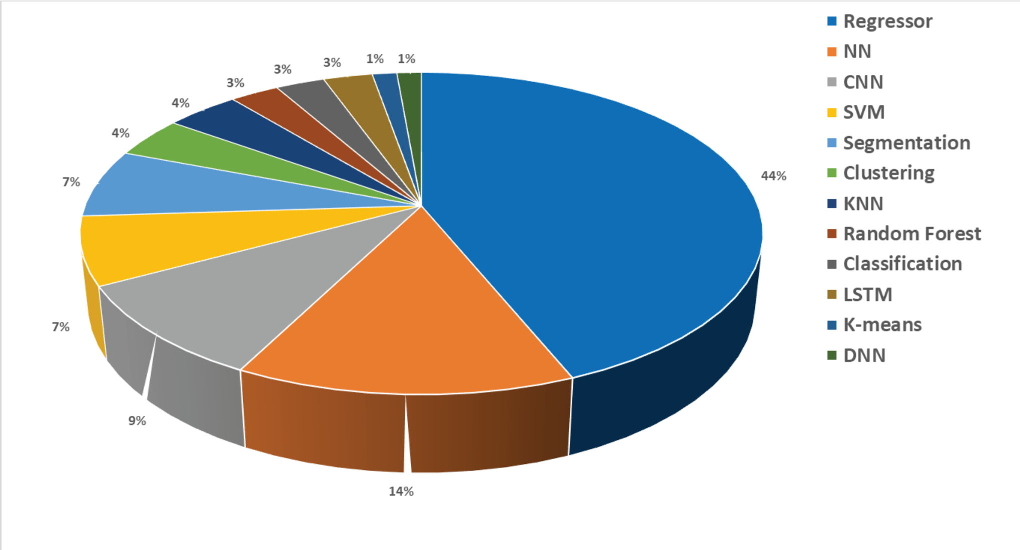

Fig. 5.2: Detailed usage distribution of methods across the entire survey

require large amount of data [95] and accurate calibration [46], [57]. Cloud cover and other weather extremities can affect the quality of data gathered [46] [48]. Another challenge is crop diversity due to geographical and environmental variations. It is difficult to obtain specific data on multiple variants of the individual crop, which is crucial for estimation [20] [57]. Expensive equipment is required for data gathering, which is a bottleneck for economical solutions [45]. Further, data gathering is subjected to several inherent problems such as blurring of images [58], limited [42], unbalanced [39], missing data [85] and complex capturing technique [108]. Certain IP, DL, and RS models provide better results. However, the data required by these models need to undergo a complex preprocessing stage which is resource intensive, and time-consuming [97] [74] [108].

6.2. Model related issues. Researchers designed several estimation models using different methods. The designed model is applicable with specific conditions or over specific crops due to inherent variations. Example RS model is suitable for rainfed crops and cannot be applied to irrigated lands on the specified ROI [100]. Also, there is no common model that fits all crops. Research is carried out around standard crops [17] such as wheat [90] [23], rice [41], cotton [80], few fruits [44] [45] [97] and vegetables [65]. This introduces a new issue of certain crops being eliminated as they are grown in limited regions or countries which needs to be addressed. Certain models such as RS, ML and DL depend on image data and focus on counting-based yield estimation [99] [44]. However, inherent image processing issues such as occlusion [53], illumination [59], duplicate count [82], geo-referencing [45] [74], and object clusters [98] are few major challenges that affect the accuracy of prediction in these models. ML, RS, and CM need a careful selection of input features. No standard algorithms or methods can be used to perform this task [105]. DL and CM simulation version have high computational complexity due to complex input data [54] [53] [74]. Certain IP, DL, and RS models provide good results with certain inputs. However, it requires a resource-intensive and time-consuming preprocessing stage to generate these inputs [108] [85]. Also, these models require expensive equipment for data capturing, preprocessing and training [45] [74]. Insufficient or missing historical yield estimates gathered using traditional techniques [102] or market studies led researchers to fill the gap using synthetic data, which may not lead to an optimal model [47] [106].

6.3. Analysis related issues. Count and weight are the major representation of yield value. CM, RS [46] and ML models produce weight-based results [93], while image processing, RS (image) and deep learning models provide counting based results [63] [99] [44]. A single model cannot handle both representations. Further, different models are designed to solve estimation problems for a particular crop. Researchers have used different evaluation metrics and input parameters to solve the problem. For example, CM and RS models are used to estimate rice yield. However, different evaluation metrics with different result values were used for result verification as per their design [41][57][89]. Hence, it isn't easy to establish a common evaluation metric with benchmark values.

7. Conclusion. The paper summarizes non-destructive approaches designed to estimate crop yield. Different models were developed based on input data and the methodology adopted. Statistical and simulation crop models were less researched as they could not incorporate various dynamic features effectively. The qualitative by-products of RS, such as NDVI, EVI, and DVI data, were extensively used in the crop and ML model to improve the accuracy of the model. Clustering and segmentation were widely used to separate ROIs in the image processing model. Pixel classification and segmentation architectures were used in the deep learning model for estimating crop yield. Most CNN and its variants, LSTM, were used to test and train the model for object detection and then proceeded towards counting. RS data was also experimented with for integration into deep architectures with histogram preprocessing.

To summarize, weight-based yield estimation was implemented by the crop model, ML model and RS model. These models were generally used for estimating yield in large geographical areas. Counting-based analysis was implemented by image processing, RS model and deep learning model using an image as a primary input. Single and a bunch of objects were explored during the counting process. But accuracy is still an open challenge due to object clutter and occlusion. R2, RMSE is widely used to analyze the accuracy of the yield estimation model. Further, there is a broad scope to harness the multimodal integration of RS image data, image processing techniques and deep learning techniques to estimate crop yield over large areas.

Acknowledgments. This work is supported by Visvesvaraya PhD Scheme, Ministry of Electronics and Information Technology (MeitY) Government of India MEITY-PHD-1394. We thank MeitY, the Government of India and Nirma University for facilitating our research work. Also, I would like to thank Dr Varsha Ganguly for her valuable suggestions in structuring the paper.

REFERENCES

[1] World Health Organization and others, *The State of Food Security and Nutrition in the World 2021: Transforming food systems for food security, improved nutrition and affordable healthy diets for all.*, Food & Agriculture Organization (2021).

[2] Roser, M., Ritchie, H. & Ortiz-Ospina, Esteban, *World population growth*,Our World In Data. (2013).

[3] Agricultural output Crop production OECD Data, http://data.oecd.org/agroutput/crop-production.htm, Accessed: Aug. 03 (2022).

[4] FAO, Food. & Others,*The future of food and agriculture–Trends and challenges.*, Annual Report, v296 pp. 1-180 (2017).

[5] Evans, L. & Fischer, R. Yield potential: its definition, measurement, and significance., *Crop Science.* volume 39, pp. 1544-1551 (1999).

[6] Johnson, M., Hsieh, W., Cannon, A., Davidson, A. & Bédard, F., *Crop yield forecasting on the Canadian Prairies by remotely sensed vegetation indices and machine learning methods.*, Agricultural And Forest Meteorology, volume 218, pp. 74-84 (2016).

[7] Chivasa, W., Mutanga, O. & Biradar, C.,*Application of remote sensing in estimating maize grain yield in heterogeneous African agricultural landscapes: a review.* International Journal Of Remote Sensing. volume 38, pp. 6816-6845 (2017).

[8] Liakos, K., Busato, P., Moshou, D., Pearson, S. & Bochtis, D., *Machine learning in agriculture: A review.* Sensors. 18, pp 2674 (2018).

[9] Chlingaryan, A., Sukkarieh, S. & Whelan, B.,*Machine learning approaches for crop yield prediction and nitrogen status estimation in precision agriculture: A review.* Computers And Electronics In Agriculture.151 pp. 61-69 (2018).

[10] Elavarasan, D., Vincent, D., Sharma, V., Zomaya, A. & Srinivasan, K.,*Forecasting yield by integrating agrarian factors and machine learning models: A survey.*, Computers And Electronics In Agriculture. volume 155 pp. 257-282 (2018). volume 147 pp. 70-90 (2018).

[11] Kamilaris, A. & Prenafeta-Boldú, F., *Deep learning in agriculture: A survey.*, Computers And Electronics In Agriculture. volume 147, pp. 70-90 (2018).

[12] Basso, B. & Liu, L.,*Seasonal crop yield forecast: Methods, applications, and accuracies.*,Advances In Agronomy. volume 154 pp. 201-255 (2019).

[13] Koirala, A., Walsh, K., Wang, Z. & McCarthy, C.,*Deep learning–Method overview and review of use for fruit detection and yield estimation.* Computers And Electronics In Agriculture. volume 162, pp. 219-234 (2019).

[14] Van Klompenburg, T., Kassahun, A. & Catal, C.,*Crop yield prediction using machine learning: A systematic literature review.*, Computers And Electronics In Agriculture. volume 177 pp. 105709 (2020).

[15] Maheswari, P., Raja, P., Apolo-Apolo, O. & Pérez-Ruiz, M.,*Intelligent fruit yield estimation for orchards using deep learning based semantic segmentation techniques—a review.*, Frontiers In Plant Science. volume 12, pp. 1247 (2021).

[16] Rashid, M., Bari, B., Yusup, Y., Kamaruddin, M. & Khan, N.,*A comprehensive review of crop yield prediction using machine learning approaches with special emphasis on palm oil yield prediction.*, IEEE Access. volume 9, pp. 63406-63439 (2021).

[17] Castro-Tanzi, S., Flores, M., Wanner, N., Dietsch, T., Banks, J., Ureña-Retana, N. & Chandler, M.,*Evaluation of a non-destructive sampling method and a statistical model for predicting fruit load on individual coffee (Coffea arabica) trees.*,Scientia Horticulturae. volume 167, pp. 117-126 (2014).

[18] Mahalanobis, P.,*Sample surveys of crop yields in India.*, Sankhyā: The Indian Journal Of Statistics. pp. 269-280 (1946).

[19] Kestur, R., Meduri, A. & Narasipura, O.,*MangoNet: A deep semantic segmentation architecture for a method to detect and count mangoes in an open orchard.*, Engineering Applications Of Artificial Intelligence. volume 77, pp. 59-69 (2019).

[20] Murthy, C., Thiruvengadachari, S., Raju, P. & Jonna, S.,*Improved ground sampling and crop yield estimation using satellite data.* International Journal Of Remote Sensing. volume 17, pp. 945-956 (1996).

[21] Singh, R., Semwal, D., Rai, A. & Chhikara, R. ,*Small area estimation of crop yield using remote sensing satellite data.*, International Journal Of Remote Sensing. volume 23, pp. 49-56 (2002).

[22] Kung, H., Kuo, T., Chen, C. & Tsai, P.,*Accuracy analysis mechanism for agriculture data using the ensemble neural network method.* Sustainability. volume 8, pp. 735 (2016).

[23] Pantazi, X., Moshou, D., Alexandridis, T., Whetton, R. & Mouazen, A.,*Wheat yield prediction using machine learning and advanced sensing techniques.* Computers And Electronics In Agriculture. volume 121, pp. 57-65 (2016).

[24] Marko, O., Brdar, S., Panić, M., Šašić, I., Despotović, D., Knežević, M. & Crnojević, V.,*Portfolio optimization for seed selection in diverse weather scenarios.* . PloS One. Volume 12, pp. 0184198 (2017).

[25] Liu, J., Goering, C. & Tian, L.,*A neural network for setting target corn yields.*, Transactions Of The ASAE. volume 44, pp. 705 (2001).

[26] Su, Y., Xu, H. & Yan, L.,*Support vector machine-based open crop model (SBOCM): Case of rice production in China.*, Saudi Journal Of Biological Sciences. volume 24, pp. 537-547 (2017).

[27] Dorj, U., Lee, M. & Yun, S.,*An yield estimation in citrus orchards via fruit detection and counting using image processing.* Computers And Electronics In Agriculture. volume 140 pp. 103-112 (2017).

[28] Amatya, S., Karkee, M., Gongal, A., Zhang, Q. & Whiting, M.,*Detection of cherry tree branches with full foliage in planar architecture for automated sweet-cherry harvesting.*,Biosystems Engineering. volume 146, pp. 3-15 (2016).

[29] Stajnko, D., Lakota, M. & Hočevar, M.,*Estimation of number and diameter of apple fruits in an orchard during the growing season by thermal imaging.*, Computers And Electronics In Agriculture. volume 42, 31-42 (2004).

[30] Wang, Q., Nuske, S., Bergerman, M. & Singh, S.,*Automated crop yield estimation for apple orchards.* Experimental Robotics. pp. 745-758 (2013).

[31] Chahbi Bellakanji, A., Zribi, M., Lili-Chabaane, Z. & Mougenot, B.,*Forecasting of cereal yields in a semi-arid area using the simple algorithm for yield estimation (SAFY) agro-meteorological model combined with optical SPOT/HRV images.* Sensors. volume 18, pp. 2138 (2018).

[32] Huang, J., Ma, H., Sedano, F., Lewis, P., Liang, S., Wu, Q., Su, W., Zhang, X. & Zhu, D.,*Evaluation of regional estimates of winter wheat yield by assimilating three remotely sensed reflectance datasets into the coupled WOFOST–PROSAIL model.* European Journal Of Agronomy. volume 102 pp. 1-13 (2019).

[33] Franch, B., Vermote, E., Skakun, S., Roger, J., Becker-Reshef, I., Murphy, E. & Justice, C.,*Remote sensing based yield monitoring: Application to winter wheat in United States and Ukraine.* International Journal Of Applied Earth Observation And Geoinformation. volume 76 pp. 112-127 (2019).

[34] Ines, A., Honda, K., Gupta, A., Droogers, P. & Clemente, R.,*Combining remote sensing-simulation modeling and genetic algorithm optimization to explore water management options in irrigated agriculture.* Agricultural Water Management. volume 83, pp. 221-232 (2006).

[35] Bannari, A., Morin, D., Bonn, F. & Huete, A.,*A review of vegetation indices.*Remote Sensing Reviews. volume 13, 95-120 (1995).

[36] Jiang, Z., Huete, A., Didan, K. & Miura, T.,*Development of a two-band enhanced vegetation index without a blue band.* Remote Sensing Of Environment. vomune 112, pp. 3833-3845 (2008).

[37] Salazar, L., Kogan, F. & Roytman, L.,*Use of remote sensing data for estimation of winter wheat yield in the United States.*, International Journal Of Remote Sensing. vomune 28, pp. 3795-3811 (2007).

[38] Gutiérrez, S., Wendel, A. & Underwood, J.,*Ground based hyperspectral imaging for extensive mango yield estimation.* Computers And Electronics In Agriculture. vomune 157, pp. 126-135 (2019).

[39] Marko, O., Brdar, S., Panić, M., Šašić, I., Despotović, D., Knežević, M. & Crnojević, V. ,*Portfolio optimization for seed selection in diverse weather scenarios.* PloS One. volume 12, pp. 0184198 (2017).

[40] Liu, J., Goering, C. & Tian, L., *A neural network for setting target corn yields.*, Transactions Of The ASAE. volume 44, pp. 705 (2001).

[41] Su, Y., Xu, H. & Yan, L.,*Support vector machine-based open crop model (SBOCM): Case of rice production in China.*, Saudi Journal Of Biological Sciences. volume 24, 537-547 (2017).

[42] Dorj, U., Lee, M. & Yun, S.,*An yield estimation in citrus orchards via fruit detection and counting using image processing.* Computers And Electronics In Agriculture. volume 140, pp. 103-112 (2017).

[43] Amatya, S., Karkee, M., Gongal, A., Zhang, Q. & Whiting, M.,*Detection of cherry tree branches with full foliage in planar architecture for automated sweet-cherry harvesting.* Biosystems Engineering. volume 146, pp. 3-15 (2016).

[44] Stajnko, D., Lakota, M. & Hočevar, M.,*Estimation of number and diameter of apple fruits in an orchard during the growing season by thermal imaging.*Computers And Electronics In Agriculture. volume 42, pp. 31-42 (2004).

[45] Wang, Q., Nuske, S., Bergerman, M. & Singh, S.,*Automated crop yield estimation for apple orchards.* Experimental Robotics. pp. 745-758 (2013).

[46] Chahbi Bellakanji, A., Zribi, M., Lili-Chabaane, Z. & Mougenot, B.,Forecasting of cereal yields in a semi-arid area using the simple algorithm for yield estimation (SAFY) agro-meteorological model combined with optical SPOT/HRV images. Sensors. volume 18, pp. 2138 (2018)

[47] Huang, J., Ma, H., Sedano, F., Lewis, P., Liang, S., Wu, Q., Su, W., Zhang, X. & Zhu, D.,*Evaluation of regional estimates of winter wheat yield by assimilating three remotely sensed reflectance datasets into the coupled WOFOST–PROSAIL model.*, European Journal Of Agronomy. volume 102, pp. 1-13 (2019).

[48] Franch, B., Vermote, E., Skakun, S., Roger, J., Becker-Reshef, I., Murphy, E. & Justice, C.*Remote sensing based yield monitoring: Application to winter wheat in United States and Ukraine.* International Journal Of Applied Earth Observation And Geoinformation. volume 76, pp. 112-127 (2019).

[49] Ines, A., Honda, K., Gupta, A., Droogers, P. & Clemente, R.*Combining remote sensing-simulation modeling and genetic algorithm optimization to explore water management options in irrigated agriculture.* Agricultural Water Management. volume 83, pp. 221-232 (2006).

[50] Bannari, A., Morin, D., Bonn, F. & Huete, A.*A review of vegetation indices.* Remote Sensing Reviews. volume 13, pp. 95-120 (1995).

[51] Jiang, Z., Huete, A., Didan, K. & Miura, T.*Development of a two-band enhanced vegetation index without a blue band.* Remote Sensing Of Environment. volume 112, pp. 3833-3845 (2008).

[52] Salazar, L., Kogan, F. & Roytman, L.*Use of remote sensing data for estimation of winter wheat yield in the United States.* International Journal Of Remote Sensing. volume 28, pp. 3795-3811 (2007).

[53] Gutiérrez, S., Wendel, A. & Underwood, J.*Ground based hyperspectral imaging for extensive mango yield estimation.* Computers And Electronics In Agriculture. volume 157, pp. 126-135 (2019).

[54] You, J., Li, X., Low, M., Lobell, D. & Ermon, S. *Deep gaussian process for crop yield prediction based on remote sensing data.* Thirty-First AAAI Conference On Artificial Intelligence. (2017)

[55] Ines, A., Das, N., Hansen, J. & Njoku, E.*Assimilation of remotely sensed soil moisture and vegetation with a crop simulation model for maize yield prediction.* Remote Sensing Of Environment. volume 138, pp. 149-164 (2013).

[56] Miao, Y., Mulla, D. & Robert, P. *Identifying important factors influencing corn yield and grain quality variability using artificial neural networks.* Precision Agriculture.volume 7, pp. 117-135 (2006).

[57] Gilardelli, C., Stella, T., Confalonieri, R., Ranghetti, L., Campos Taberner, M., Garcia-Haro, F. & Boschetti, M *Downscaling rice yield simulation at sub-field scale using remotely sensed LAI data.*European Journal Of Agronomy. volume 103, pp. 108-116 (2019).

[58] Ramos, P., Prieto, F., Montoya, E. & Oliveros, C.*Automatic fruit count on coffee branches using computer vision.* Computers And Electronics In Agriculture. volume 137, pp. 9-22 (2017).

[59] Sengupta, S. & Lee, W.*Identification and determination of the number of immature green citrus fruit in a canopy under different ambient light conditions.* Biosystems Engineering. volume 117, pp. 51-61 (2014).

[60] Guerif, M. & Duke, C.*Calibration of the SUCROS emergence and early growth module for sugar beet using optical remote sensing data assimilation.* European Journal Of Agronomy. volume 9, pp. 127-136 (1998).

[61] Singh, R., Goyal, R., Saha, S. & Chhikara, R.*Use of satellite spectral data in crop yield estimation surveys.* International Journal Of Remote Sensing. volume 13, pp. 2583-2592 (1992).

[62] Fang, H., Liang, S. & Hoogenboom, G.*Integration of MODIS LAI and vegetation index products with the CSM–CERES–Maize model for corn yield estimation.* International Journal Of Remote Sensing. volume 32, pp. 1039-1065 (2011).

[63] Bargoti, S. & Underwood, J.*Deep fruit detection in orchards.* 2017 IEEE International Conference On Robotics And Automation (ICRA). pp. 3626-3633 (2017).

[64] Wang, A., Tran, C., Desai, N., Lobell, D. & Ermon, S.*Deep transfer learning for crop yield prediction with remote sensing data.* Proceedings Of The 1st ACM SIGCAS Conference On Computing And Sustainable Societies. pp. 1-5 (2018).

[65] Senthilnath, J., Dokania, A., Kandukuri, M., Ramesh, K., Anand, G. & Omkar, S.*Detection of tomatoes using spectral-spatial methods in remotely sensed RGB images captured by UAV.* Biosystems Engineering. volume 146, pp. 16-32 (2016).

[66] EarthExplorer,*https://earthexplorer.usgs.gov/* , Accessed: August. 04 (2022).

[67] AMSR-E Overview National Snow and Ice Data Center,*https://nsidc.org/data/amsre/* , Accessed: June 12 (2022).

[68] IEM: ISU Soil Moisture Network. *https://mesonet.agron.iastate.edu/agclimate/*, Accessed December. 15 (2021).

[69] USDA Open Data Catalog, *https://www.usda.gov/content/usda-open-data-catalog*, Accessed: June. 12 (2022).

[70] LP DAAC Data, *https://lpdaac.usgs.gov/data/*, Accessed: July. 15 (2022).

[71] National Geospatial Center of Excellence (NGCE) | NRCS. https://www.nrcs.usda.gov/wps/portal/nrcs/main/ national/ngce/. Accessed December 23 (2021).

[72] MODIS Web.,*https://modis.gsfc.nasa.gov/data/*,Accessed: June. 25 (2022).

[73] Syngenta Crop Challenge 2021,*https://www.ideaconnection.com/syngenta-crop-challenge/challenge.php/2018*, Accessed: February. 16 (2021).

[74] Variety Testing: Soybeans in Illinois Index,*http://vt.cropsci.illinois.edu/soybean.html* ,Accessed: March. 5 (2022).

[75] ACPF Downloads, Geographic Information Systems, Iowa State University, *https://www.gis.iastate.edu/gisf/projects/acpf* ,Accessed: March. 16 (2022).

[76] Soil Survey & Digital Soil Data: ISPAID , Soil and Land Use , *https://www.extension.iastate.edu/soils/ispaid*, Accessed: February. 25 (2022).

[77] A. Meduri The MangoNet Semantic Dataset 2021.*https://github.com/avadesh02/MangoNet-Semantic-Dataset* Ac-

cessed: January 29 (2022)

[78] COCO - Common Objects in Context.,*https://cocodataset.org/home*, Accessed: October. 27 (2021).

[79] schmitt-muc, SEN12MS Toolbox. 2021, *https://github.com/schmitt-muc/SEN12MS*, Accessed: October. 27 (2021).

[80] Feng, A., Zhou, J., Vories, E., Sudduth, K. & Zhang, M.*Yield estimation in cotton using UAV-based multi-sensor imagery.*Biosystems Engineering. volume 193 pp. 101-114 (2020).

[81] Haden, A., Burnham, M., Yang, W. & DeLucia, E. *Comparative establishment and yield of bioenergy sorghum and maize following pre–emergence waterlogging.* Center for Advanced Bioenergy (2021).

[82] Kestur, R., Meduri, A. & Narasipura, O.*MangoNet: A deep semantic segmentation architecture for a method to detect and count mangoes in an open orchard.* Engineering Applications Of Artificial Intelligence. volume 77, pp. 59-69 (2019).

[83] Charles-Edwards, D.*Modelling plant growth and development.* (1986).

[84] Van Diepen, C., Wolf, J., Van Keulen, H. & Rappoldt, C.*WOFOST: a simulation model of crop production.* Soil Use And Management. volume 5, pp. 16-24 (1989),

[85] Inman-Bamber, N.*A growth model for sugar-cane based on a simple carbon balance and the CERES-Maize water balance.* South African Journal Of Plant And Soil. volume 8, pp. 93-99 (1991).

[86] Spitters, C., Van Keulen, H. & Van Kraalingen, D.*A simple and universal crop growth simulator: SUCROS87* Simulation And Systems Management In Crop Protection. pp. 147-181 (1989).

[87] Launay, M. & Guerif, M.*Assimilating remote sensing data into a crop model to improve predictive performance for spatial applications.* Agriculture, Ecosystems & Environment. volume 111, pp. 321-339 (2005).

[88] Xevi, E., Gilley, J. & Feyen, J.*Comparative study of two crop yield simulation models.* Agricultural Water Management. volume 30, pp. 155-173 (1996).

[89] Pirmoradian, N. & Sepaskhah, A.*A very simple model for yield prediction of rice under different water and nitrogen applications. Biosystems Engineering.* Volume 93, pp. 25-34 (2006).

[90] Singh, A., Tripathy, R. & Chopra, U.*Evaluation of CERES-Wheat and CropSyst models for water–nitrogen interactions in wheat crop. Agricultural Water Management.* volume 95, pp. 776-786 (2008).

[91] Han, C., Zhang, B., Chen, H., Liu, Y. & Wei, Z.*Novel approach of upscaling the FAO AquaCrop model into regional scale by using distributed crop parameters derived from remote sensing data.* Agricultural Water Management. volume 240, pp. 106288 (2020).

[92] Xue, J. & Su, B. *Significant remote sensing vegetation indices: A review of developments and applications.* Journal Of Sensors. volume 2017 (2017),

[93] Barnett, T. & Thompson, D.*The use of large-area spectral data in wheat yield estimation.* Remote Sensing Of Environment. volume 12, pp. 509-518 (1982).

[94] Barnett, T. & Thompson, D.*Large-area relation of Landsat MSS and NOAA-6 AVHRR spectral data to wheat yields.* Remote Sensing Of Environment. volume 13, pp. 277-290 (1983).

[95] Ali, I., Cawkwell, F., Dwyer, E. & Green, S.*Modeling managed grassland biomass estimation by using multitemporal remote sensing data—A machine learning approach.* IEEE Journal Of Selected Topics In Applied Earth Observations And Remote Sensing. volume 10, pp. 3254-3264 (2016).

[96] He, M., Kimball, JS, Maneta, M., Maxwell, B., Moreno, A., Beguería, S. & Wu, m.*Regional crop gross primary productivity and yield estimation using fused landsat MODIS data.* Remote Sensing. volume 10, pp. 372 (2018).

[97] Maldonado Jr, W. & Barbosa, J.*Automatic green fruit counting in orange trees using digital images.* Computers And Electronics In Agriculture. volume 127, pp. 572-581 (2016).

[98] Nuske, S., Wilshusen, K., Achar, S., Yoder, L., Narasimhan, S. & Singh, S.*Automated visual yield estimation in vineyards.* Journal Of Field Robotics. volume 31,pp. 837-860 (2014).

[99] Liu, S., Marden, S. & Whitty, M. *Towards automated yield estimation in viticulture.* Proceedings Of The Australasian Conference On Robotics And Automation, Sydney, Australia. volume 24, pp. 2-6 (2013).

[100] Sakamoto, T.*Incorporating environmental variables into a MODIS-based crop yield estimation method for United States corn and soybeans through the use of a random forest regression algorithm.* ISPRS Journal Of Photogrammetry And Remote Sensing. volume 160, pp. 208-228 (2020).

[101] Drummond, S., Sudduth, K., Joshi, A., Birrell, S. & Kitchen, N.*Statistical and neural methods for site–specific yield prediction.* Transactions Of The ASAE. volume 46,pp. 5 (2003).

[102] Crane-Droesch, A.*Machine learning methods for crop yield prediction and climate change impact assessment in agriculture.* Environmental Research Letters. volume 13, pp. 114003 (2018).

[103] Zhang, L., Zhang, J., Kyei-Boahen, S., Zhang, M. & Others *Simulation and prediction of soybean growth and development under field conditions.* Am-Euras J Agr Environ Sci. volume 7, pp. 374-385 (2010).

[104] Veenadhari, S., Misra, B. & Singh, C. *Machine learning approach for forecasting crop yield based on climatic parameters.* 2014 International Conference On Computer Communication And Informatics. pp. 1-5 (2014).

[105] Irmak, A., Jones, J., Batchelor, W., Irmak, S., Boote, K. & Paz, J.*Artificial neural network model as a data analysis tool in precision farming.* Transactions Of The ASABE. volume 49, pp. 2027-2037 (2006).

[106] Rahnemoonfar, M. & Sheppard, C. *Deep count: fruit counting based on deep simulated learning.* Sensors. volume 17, pp. 905 (2017).

[107] Khaki, S. & Wang, L. *Crop yield prediction using deep neural networks.* Frontiers In Plant Science. volume 10, pp. 621 (2019).

[108] Maimaitijiang, M., Sagan, V., Sidike, P., Hartling, S., Esposito, F. & Fritschi, F. *Soybean yield prediction from UAV using multimodal data fusion and deep learning.* Remote Sensing Of Environment. volume 237, pp. 111599 (2020).

Edited by: Katarzyna Wasielewska
Received: Jun 28, 2022
Accepted: Aug 12, 2022

AIMS AND SCOPE

The area of scalable computing has matured and reached a point where new issues and trends require a professional forum. SCPE will provide this avenue by publishing original refereed papers that address the present as well as the future of parallel and distributed computing. The journal will focus on algorithm development, implementation and execution on real-world parallel architectures, and application of parallel and distributed computing to the solution of real-life problems. Of particular interest are:

Expressiveness:
- high level languages,
- object oriented techniques,
- compiler technology for parallel computing,
- implementation techniques and their efficiency.

System engineering:
- programming environments,
- debugging tools,
- software libraries.

Performance:
- performance measurement: metrics, evaluation, visualization,
- performance improvement: resource allocation and scheduling, I/O, network throughput.

Applications:
- database,
- control systems,
- embedded systems,
- fault tolerance,
- industrial and business,
- real-time,
- scientific computing,
- visualization.

Future:
- limitations of current approaches,
- engineering trends and their consequences,
- novel parallel architectures.

Taking into account the extremely rapid pace of changes in the field SCPE is committed to fast turnaround of papers and a short publication time of accepted papers.

INSTRUCTIONS FOR CONTRIBUTORS

Proposals of Special Issues should be submitted to the editor-in-chief.

The language of the journal is English. SCPE publishes three categories of papers: overview papers, research papers and short communications. Electronic submissions are preferred. Overview papers and short communications should be submitted to the editor-in-chief. Research papers should be submitted to the editor whose research interests match the subject of the paper most closely. The list of editors' research interests can be found at the journal WWW site (`http://www.scpe.org`). Each paper appropriate to the journal will be refereed by a minimum of two referees.

There is no a priori limit on the length of overview papers. Research papers should be limited to approximately 20 pages, while short communications should not exceed 5 pages. A 50–100 word abstract should be included.

Upon acceptance the authors will be asked to transfer copyright of the article to the publisher. The authors will be required to prepare the text in LaTeX 2_ε using the journal document class file (based on the SIAM's `siamltex.clo` document class, available at the journal WWW site). Figures must be prepared in encapsulated PostScript and appropriately incorporated into the text. The bibliography should be formatted using the SIAM convention. Detailed instructions for the Authors are available on the SCPE WWW site at `http://www.scpe.org`.

Contributions are accepted for review on the understanding that the same work has not been published and that it is not being considered for publication elsewhere. Technical reports can be submitted. Substantially revised versions of papers published in not easily accessible conference proceedings can also be submitted. The editor-in-chief should be notified at the time of submission and the author is responsible for obtaining the necessary copyright releases for all copyrighted material.